Macromolecules **1998,** *31,* 1779−1790

Correlation of Model Compounds and Laterally Attached Side-Chain Liquid-Crystalline Polynorbornenes with an 11-Carbon Spacer

Coleen Pugh,*,† Jun Shao,† Jason J. Ge,‡ and Stephen Z. D. Cheng‡

Macromolecular Science and Engineering Center, Department of Chemistry, University of Michigan, Ann Arbor, Michigan 48109-1055, and Department of Polymer Science, University of Akron, Akron, Ohio 44329-3909

Received October 27, 1997; Revised Manuscript Received December 22, 1997

ABSTRACT: Poly{5-[[[11′-[2″,5″-bis[2-(3′-fluoro-4′-*n*-alkoxyphenyl)ethynyl]phenyl]undecyl]oxy]carbonyl]-bicyclo[2.2.1]hept-2-ene}s exhibit an enantiotropic nematic mesophase when $n = 2-12$. In contrast to the corresponding reference polymers with a 1-carbon spacer, none of these polymers with an 11-carbon spacer crystallize if their molecular weight is sufficiently high. Although the corresponding 1,4-bis[(3′-fluoro-4′-*n*-alkoxyphenyl)ethynyl]-2-undecylbenzenes exhibit only a monotropic nematic mesophase when $n = 2$, 4, 6−11, their isotropization temperatures are nearly identical to those of the polynorbornenes, and they are therefore appropriate models of the polymers. The polymers ($DP_n = 14-158$, pdi = 1.14−1.37) were prepared by ring-opening metathesis polymerization of 5-{[[11′-[2″,5″-bis[2-(3′-fluoro-4′-*n*-alkoxyphenyl)ethynyl]phenyl]undecyl]oxy]carbonyl}bicyclo[2.2.1]hept-2-enes in THF using Mo(CHCMe$_2$-Ph)(N-2,6-^{i}Pr$_2$Ph)(O^{t}Bu)$_2$ as the initiator. Their thermotropic behavior becomes independent of molecular weight at approximately 30 repeat units.

Introduction

Low molar mass liquid crystals (LMMLCs) based on extended mesogens that are symmetrically disubstituted with long *n*-alkoxy substituents tend to exhibit smectic C (s_C) mesophases.[1] For example, 1,4-bis[(3′-fluoro-4′-*n*-alkoxyphenyl)ethynyl]benzenes exhibit a smectic C−nematic (s_C−n) phase sequence when $n = 6-12$.[2,3] On the basis of this tendency of symmetrically disubstituted, extended mesogens to exhibit s_C mesophases, we have proposed that side-chain liquid-crystalline polymers (SCLCPs) with laterally attached (vs terminally attached) mesogens offer an ideal architecture for obtaining s_C and chiral smectic C (s_C*) mesophases.[4] That is, lateral attachment allows extended mesogens to be incorporated as side chains to a polymer backbone without disrupting their symmetrical disubstitution. However, most laterally attached SCLCPs exhibit only nematic mesophases,[3,5−9] presumably because the large extended mesogens impose steric constraints on the small structural unit of the polymer backbone. This forces the backbone into an extended helical conformation, with the mesogens jacketing it;[7,8] the centers of mass of the mesogens are therefore staggered, which corresponds to a nematic mesophase. However, we recently demonstrated that both nematic LMMLCs and polynorbornenes with laterally attached 1,4-bis[(4′-*n*-alkoxybenzoyl)oxy]benzene mesogens can be forced to order into smectic layers by terminating their *n*-alkoxy substituents with either immiscible fluorocarbon[10] or immiscible siloxane[11] segments.

To determine the effect of incorporating a mesogen that exhibits a s_C−n or s_C−i phase sequence into a laterally attached architecture without altering any other structural variables, we first replaced the mesogen of a well-defined reference polymeric system with a 1,4-bis[(3′-fluoro-4′-*n*-alkoxyphenyl)ethynyl]benzene mesogen.[3] The reference poly{5-[[[2′,5′-bis[(4″-*n*-alkoxybenzoyl)oxy]benzyl]oxy]carbonyl]bicyclo[2.2.1]hept-2-ene}s were the only well-defined laterally attached SCLCPs prepared at the time.[12] However, short spacers generally preclude smectic layering.[13] In addition, the mesogen density affects the phase(s) formed by liquid-crystalline polynorbornenes. For example, polynorbornenes with two terminally attached *p*-cyanobiphenyl mesogens per repeat unit form s_A mesophases when the spacer is sufficiently long,[14] whereas the corresponding polynorbornenes with only one mesogen per repeat unit form nematic mesophases.[15]

Since short spacers generally preclude smectic layering,[13] it was not surprising that none of the poly{5-[[[2′,5′-bis[2-(3′-fluoro-4′-*n*-alkoxyphenyl)ethynyl]benzyl]-oxy]carbonyl]bicyclo[2.2.1]hept-2-ene}s exhibit a s_C mesophase.[3] Now that we have systematically determined the effect of changing only the laterally attached mesogen from one that forms a nematic mesophase to one that tends to exhibit a s_C−n phase sequence, we will determine the effect of increasing the spacer length in order to favor smectic mesophase formation and, if necessary, the effect of doubling the mesogen density along the polynorbornene backbone. As outlined in Chart 1, the poly{5-[[[2′,5′-bis[2-(3′-fluoro-4′-*n*-alkoxyphenyl)ethynyl]benzyl]oxy]carbonyl]bicyclo[2.2.1]hept-2-ene}s with a 1-carbon spacer are now our reference polymers. This paper will compare their thermotropic behavior to that of the title polymers with an 11-carbon spacer (Chart 1). In addition, we have determined the thermotropic behavior of {2,5-bis[(3′-fluoro-4′-*n*-alkoxyphenyl)ethynyl]phenyl}undecanes as possible models of the title polymers. These LMMLCs are based on identical mesogens with identical *n*-alkoxy substituents and are further substituted with a lateral undecyl group to mimic the 11-carbon spacer of the polymers. Similarly, 1,4-bis[(3′-fluoro-4′-*n*-alkoxyphenyl)ethynyl]toluenes, which contain a lateral methyl substituent, mimic the thermotropic behavior of the reference polymers with a benzylic spacer.

---

* Author to whom correspondence should be addressed.

† University of Michigan.

‡ University of Akron.

S0024-9297(97)01573-8 CCC: $15.00

Chart 1. Side-Chain Liquid-Crystalline Polynorbornenes and the Corresponding Low Molar Mass Model Compounds Containing a Mesogen That Tends To Exhibit a s$_C$−n Phase Sequence

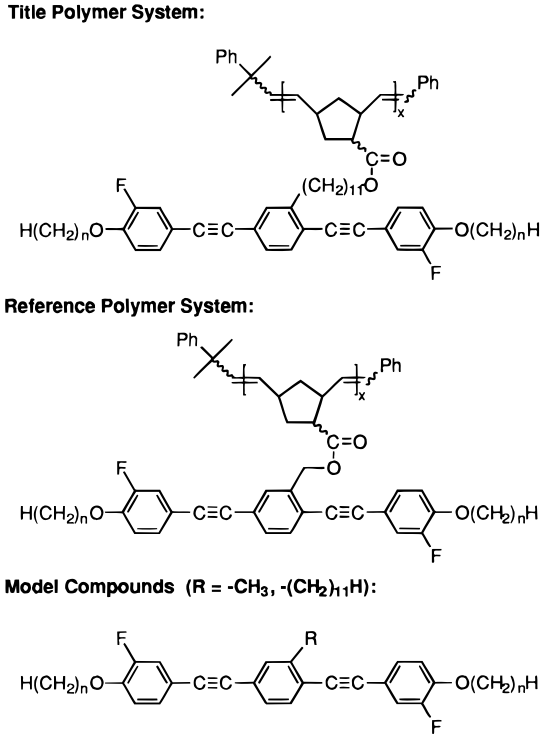

Scheme 1. Synthesis of the {2,5-Bis[(3′-fluoro-4′-*n*-alkoxyphenyl)ethynyl]phenyl}undecane Model Compounds (*n* = 1−12)

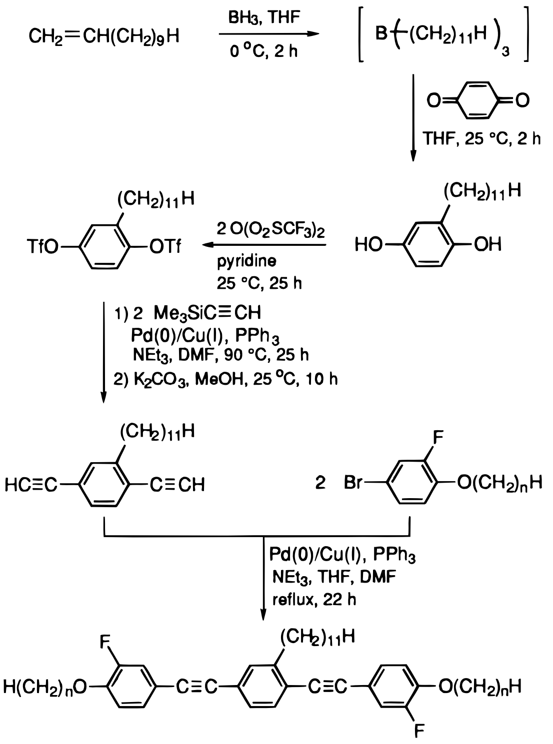

Table 1. Thermal Transitions and Thermodynamic Parameters of {2,5-Bis[(3′-fluoro-4′-*n*-alkoxyphenyl)ethynyl]phenyl}undecanes[a]

	phase transitions, °C (Δ*H*, kJ/mol)	
n	heating	cooling
1	k 62 (34.8) i	i
2	k 39 (5.34) k 51 (27.6) [n 47 (0.86)] i	i 45 (0.90) n
3	k 77 (33.0) i	i 35 (37.3) k
4	k 67 (28.2) [n 47 (0.66)] i	i 44 (0.69) n 28 (26.1) k
5	k 63 (37.8) i	i 24 (31.7) k
6	k 65 (47.5) [n 47 (0.35)][b] i	i 46 (0.94) n 22 (50.8) k
7	k 47 (40.7) [n 46 (0.89)] i	i 44 (0.89) n 11 (29.7) k
8	k 52 (44.1) [n 50 (0.90)][b] i	i 48 (1.42) n −6 (30.4) k
9	k 60 (43.2) [n 48 (0.60)][b] i	i 47 (1.18) n 27 (37.2) k
10	k 58 (66.4) [n 53 (1.84)] i	i 53 (1.89) n 29 (55.4) k
11	k 60 (80.1) [n 52 (1.80)] i	i 51 (1.74) n 26 (39.8) k
12	k 49 (44.2) n 53 (1.77) i	i 50 (1.73) n 24 (37.5) k

[a] k = crystalline, n = nematic, i = isotropic [monotropic]. [b] Enthalpy change of monotropic transition underestimated because recrystallization was not completely suppressed.

Results and Discussion

Synthesis and Thermotropic Behavior of 1,4-Bis[(3′-fluoro-4′-*n*-alkoxyphenyl)ethynyl]-2-undecylbenzenes. The 1,4-bis[(3′-fluoro-4′-*n*-alkoxyphenyl)ethynyl]-2-undecylbenzene model compounds were synthesized by the route outlined in Scheme 1. As described previously for other alkylhydroquinones,[16] 2-undecyl-1,4-hydroquinone was synthesized in 81−90% yield by reductive alkylation of hydroquinone using triundecylborane; triundecylborane was generated in situ by hydroboration of 1-undecene with borane. This reductive alkylation has also been used to prepare laterally attached SCLCPs based on 1,4-bis(benzoyloxy)benzene mesogens.[6] 2-Undecyl-1,4-hydroquinone was then reacted with 2 equiv of triflic anhydride to generate the aryl bistriflate,[17] which was coupled with 2 equiv of (trimethylsilyl)acetylene using $PdCl_2(PPh_3)_2$/CuI as the catalyst in the presence of triphenylphosphine and triethylamine in DMF at 90 °C.[17,18] After deprotection of the trimethylsilyl groups, the bisacetylene was coupled with 2 equiv of the appropriate 1-bromo-3-fluoro-4-*n*-alkoxybenzene using the same Pd(0)/Cu(I) catalyst system used to prepare the bisacetylene. This was the lowest yield step in the synthesis; we did not optimize it further.

Table 1 summarizes the thermal transitions obtained on heating and on cooling the model compounds. The data obtained on heating are from samples that are at thermodynamic equilibrium and represent samples crystallized from solution and/or from the melt. However, many of the compounds do not recrystallize from the melt to the most thermodynamically stable phase within the time scale of the differential scanning calorimetry (DSC) experiment without further annealing. For example, the methoxy derivative does not recrystallize on cooling or by annealing at elevated temperature for 30 min, although it does recrystallize at 36 °C on reheating or after annealing at room temperature for several days. The ethoxy, nonyloxy, and undecyloxy derivatives tend to be polymorphic as crystallized from the melt but also reach thermodynamic equilibrium after annealing at room temperature for several days. Nevertheless, many of the compounds either achieve equilibrium (*n* = 3, 5, 6, 10, 12) or are close to equilibrium (*n* = 4, 7, 8) upon cooling from the isotropic melt at 10 °C/min.

Only the *n* = 12 derivative exhibits an enantiotropic nematic mesophase. The nematic mesophase is confirmed by the representative polarized optical micrograph shown in Figure 1.[19] With the exception of the *n* = 3,4 derivatives which are only crystalline, the nematic mesophase of all of the other model compounds is monotropic and is exhibited only on cooling. Nevertheless, the temperature of isotropization observed on

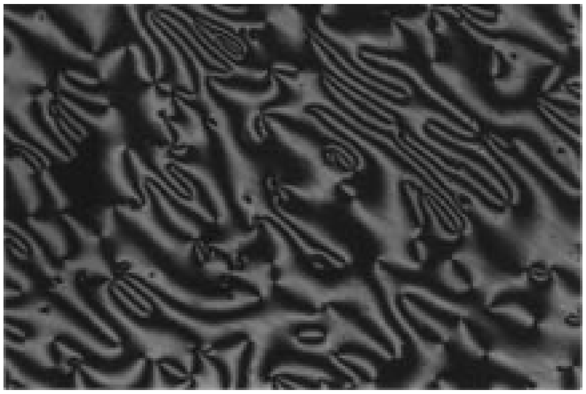

Figure 1. Polarized optical micrograph (200×) observed on cooling {2,5-bis[(3′-fluoro-4′-*n*-heptoxyphenyl)ethynyl]phenyl}-undecane (*n* = 7 model compound) from the isotropic melt; 45.5 °C, schlieren nematic texture.

heating the nematic mesophase is essentially constant as a function of the length of the *n*-alkoxy substituents, as is the temperature of the isotropic−nematic transition observed on cooling. The temperatures of melting and crystallization are also similar regardless of the length of the *n*-alkoxy substituents but vary with a slight odd−even alternation.

Synthesis and Thermotropic Behavior of Monomers. The norbornene monomers laterally attached with 1,4-bis[(3′-fluoro-4′-*n*-alkoxyphenyl)ethynyl]benzene mesogens through an 11-carbon spacer were synthesized by a route similar to that used to synthesize the model compounds. As outlined in Scheme 2, the alcohol of 10-undecenyl alcohol was first protected as an acetate group, and the resulting 10-undecenyl acetate was then hydroborated with borane and used to reductively alkylate hydroquinone. 11-(2′,5′-Dihydroxyphenyl)undecyl acetate was then reacted with 2 equiv of triflic anhydride to generate the aryl bistriflate,[17] which was coupled with 2 equiv of (trimethylsilyl)-acetylene catalyzed by Pd(0)/Cu(I).[17,18] Both the acetate and trimethylsilyl groups were deprotected using potassium carbonate in methanol. The resulting 11-[2′,5′-bis(acetylene)phenyl]undecanol was then coupled with 2 equiv of the appropriate 1-bromo-3-fluoro-4-*n*-alkoxybenzene; this Pd(0)/Cu(I)-catalyzed coupling reaction was again the low yield step in the synthesis. The final monomers were prepared by esterification of each of the 11-{2′,5′-bis[2-(3″-fluoro-4″-*n*-alkoxyphenyl)ethynyl]-phenyl}undecanols with bicyclo[2.2.1]hept-2-ene-5-carboxyl chloride.

Scheme 2. Synthesis of the 5-{[11′-[2″,5″-Bis[2-[(3′-fluoro-4′-*n*-alkoxyphenyl)ethynyl]phenyl]undecyl]-oxy]carbonyl}bicyclo[2.2.1]hept-2-ene Monomers (*n* = 1−12)

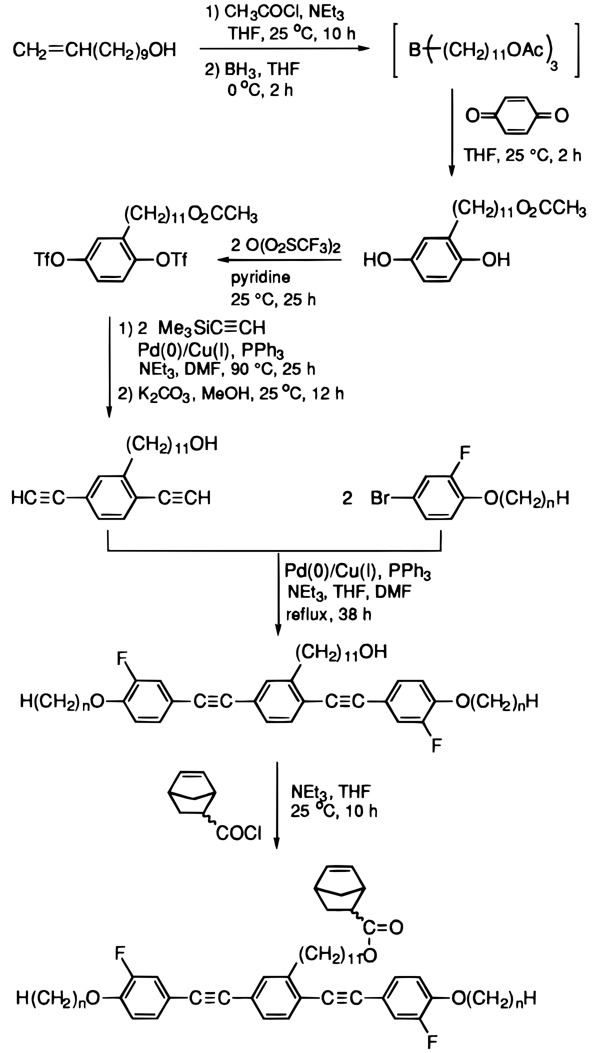

Table 2. Thermal Transitions and Thermodynamic Parameters of 5-{[[11′-[2″,5″-Bis[2-(3′-fluoro-4′-*n*-alkoxyphenyl)ethynyl]phenyl]undecyl]oxy]carbonyl}-bicyclo[2.2.1]hept-2-enes (Monomers)[a]

		phase transitions, °C (Δ*H*, kJ/mol)	
n	% endo	heating	cooling
1	78	i	i
2	85	k 45 (18.1) k 48 (26.9) [n 8 (0.77)] i	i 4 (0.87) n
3	73	k 47 (34.8) i	i
4	75	k 44 (35.2) [n 8 (0.73)] i	i 3 (1.11) n
5	67	k 38 (41.7) [n 3 (0.45)] i	i −1 (0.74) n
6	67	n 8 (0.78) i	i 5 (0.88) n
7	57	k 36 (45.7) [n 14 (0.92)] i	i 8 (1.20) n
8	67	k 36 (49.8) [n 23 (1.91)] i	i 18 (1.80) n
9	50	k 58 (66.8) [n 24 (0.73)] i	i 19 (1.68) n
10	60	k 42 (54.9) [n 31 (1.39)] i	i 26 (2.32) n
11	67	k 46 (58.3) [n 27 (1.10)] i	i 25 (2.33) n
12	67	k 39 (52.7) [n 34 (1.38)] i	i 30 (1.66) n

[a] k = crystalline, n = nematic, i = isotropic [monotropic].

The equilibrium thermotropic behavior of the 5-{[[11′-[2″,5″-bis[2-(3′-fluoro-4′-*n*-alkoxyphenyl)ethynyl]phenyl]-undecyl]oxy]carbonyl}bicyclo[2.2.1]hept-2-ene monomers is summarized in Table 2. The monomer with *n* = 1 is a viscous isotropic liquid, with no detectable transition from −30 to +80 °C. With the exception of the *n* = 6 monomer which does not crystallize from either solution or the melt, all of the other monomers are crystalline. However, none of these monomers recrystallize on cooling at 10 °C/min. The *n* = 3 monomer recrystallizes slightly on reheating and completely after annealing at 40 °C for 30 min or at room temperature for a few days. With the exception of the *n* = 2 and *n* = 8 monomers, all of the other crystalline monomers crystallize at least partially on reheating, although it may not be to the most thermodynamically stable crystalline phase (*n* = 7, 10, 12). These monomers generally reach thermodynamic equilibrium by annealing at room temperature for several days. However, the *n* = 7,8 monomers require annealing at room temperature for more than 1 month to recrystallize completely into the most thermodynamically stable crystalline phase.

With the exception of the *n* = 1 and *n* = 3 monomers, all of the monomers presumably exhibit a monotropic

Scheme 3. Ring-Opening Metathesis Polymerization of 5-{[11′-[2″,5″-Bis[2-[(3′-fluoro-4′-*n*-alkoxyphenyl)-ethynyl]phenyl]undecyl]oxy]carbonyl}bicyclo[2.2.1]-hept-2-ene Monomers ($n = 1-12$)

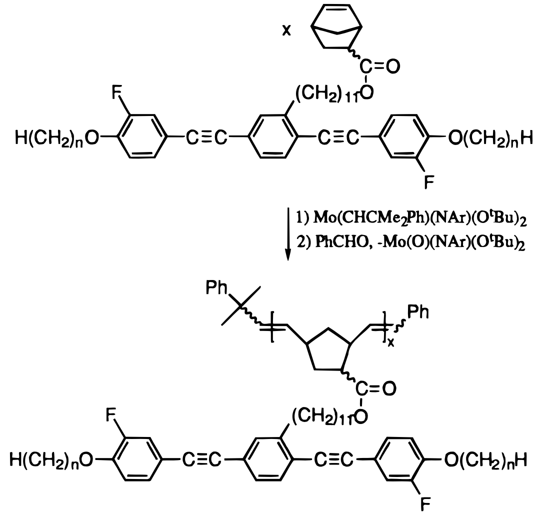

Table 3. Polymerization of 5-{[[11′-[2″,5″-Bis[2-(3′-fluoro-4′-*n*-alkoxyphenyl)ethynyl]phenyl]undecyl]oxy]carbonyl}-Bicyclo[2.2.1]hept-2-enes and Characterization of the Resulting Polymers[a]

	%		yield	theoretical	GPC		
n	endo	$[M]_0/[I]_0$	(%)	$M_n \times 10^{-4}$	$M_n \times 10^{-4}$	DP_n	pdi
1	78	50	88	3.33	4.42	66	1.17
2	85	50	90	3.46	3.63	51	1.29
3	73	42	89	3.03	2.58	36	1.19
4	75	50	92	3.74	3.67	49	1.13
5	67	50	86	3.88	5.34	68	1.14
6	67	50	89	4.03	3.54	44	1.21
7	57	50	91	4.17	4.23	50	1.18
8	67	50	88	4.31	4.17	49	1.16
9	50	5	90	0.445	1.29	14	1.20
9	50	20	86	1.78	1.54	17	1.11
9	50	35	86	3.11	2.41	27	1.26
9	0	50	92	4.45	3.59	40	1.16
9	50	55	85	4.89	5.20	58	1.19
9	50	80	73	7.11	8.08	91	1.37
9	50	100	91	8.89	14.0	158	1.37
10	60	50	87	4.59	4.42	48	1.13
11	67	42	86	3.97	3.51	37	1.15
12	67	50	85	4.87	4.43	45	1.20

[a] Polymerized in THF at room temperature for 2 h; number average molecular weight (M_n), number-average degree of polymerization (DP_n), and polydispersity (pdi = M_w/M_n) determined by gel permeation chromatography (GPC) relative to polystyrene using the mean of RI and UV detectors.

($n = 2$, 4, 5, 7−12) or enantiotropic ($n = 6$) nematic mesophase. That is, the nematic−isotropic transition is well below room temperature when $n \leq 7$ and is therefore difficult to observe by polarized optical microscopy. Nevertheless, since the monomers with longer *n*-alkoxy substituents exhibit identifiable nematic mesophases and since the nematic mesophases of LMMLCs are generally destabilized by increasing the substituent length whereas smectic phases are stabilized,[1] we are confident that the liquid-crystalline phases of the shorter homologues are also nematic.

Comparison of Tables 1 and 2 demonstrates that the nematic mesophases of both the model compounds and the monomers tend to be monotropic and observed only on cooling. Neither the monomers nor model compounds with $n = 1$ and $n = 3$ exhibit a nematic mesophase; the $n = 5$ monomer exhibits a monotropic nematic phase, although the n=5 model compound does not. Both the melting and isotropization transitions of the monomers are depressed relative to those of the model compounds, although isotropization is depressed more than melting in all cases where both transitions are observed. Therefore, termination of the *n*-undecyl lateral substituent on the 1,4-bis[(3′-fluoro-4′-*n*-alkoxyphenyl)ethynyl]-2-undecylbenzenes with a bulky norbornyl carboxylate destabilizes the nematic mesophase more than the crystalline phase.

Synthesis and Thermotropic Behavior of Polymers. As shown in Scheme 3, the 5-{[[11′-[2″,5″-bis[2-(3′-fluoro-4′-*n*-alkoxyphenyl)ethynyl]phenyl]undecyl]oxy]carbonyl}bicyclo[2.2.1]hept-2-enes were polymerized by ring-opening metathesis polymerization (ROMP) in THF at room temperature using $Mo(CHCMe_2Ph)(N\text{-}2,6\text{-}{}^iPr_2Ph)(O^tBu)_2$ as the initiator. The results of the polymerizations are summarized in Table 3. With the exception of the polymerizations of the $n = 9$ monomer, all of the polymerizations were performed using $[M]_0/[I]_0 \approx 50$. According to the GPC-determined molecular weights relative to polystyrene, all of the resulting polymers contain at least 36 repeat units. We also polymerized the $n = 9$ monomer with a range of chain lengths ($DP_n = 14-158$) in order to confirm that the thermotropic behavior of these laterally attached side-chain liquid-crystalline polynorbornenes based on an 11-carbon spacer is independent of molecular weight when $DP_n > 25$. In addition, we synthesized a polymer from the $n = 9$ monomer composed of only the exo isomer in order to compare its thermotropic behavior to the polymers based on monomers containing a mixture of endo and exo isomers. With the exception of the two highest molecular weight $n = 9$ polymers ($DP_n = 91$, 158; pdi = $M_w/M_n = 1.37$), all of the polymers have relatively narrow polydispersities (pdi = 1.11−1.29). As with the reference polymers with a 1-carbon spacer,[3] this indicates that chain transfer by secondary metathesis at the acetylene groups is not detectable at these molecular weights.

The thermotropic behavior of the title polymers is summarized in Table 4. In contrast to the reference polymer with a 1-carbon spacer, the title polymer with methoxy substituents and an 11-carbon spacer is not liquid crystalline. However, all of the other polymers with $n = 2-12$ exhibit an enantiotropic nematic mesophase. Figure 2 presents the differential scanning calorimetry (DSC) traces of the polymers observed on heating and on cooling at 10 °C/min. The heating scans are representative of freshly precipitated polymers, as well as of their second and subsequent heating scans. All of the polymers undergo a distinct glass transition upon heating, and those with $n = 2-12$ exhibit a sharp endotherm at higher temperature due to the nematic−isotropic transition. In contrast to the freshly precipitated reference polymers with a 1-carbon spacer, these polymers with an 11-carbon spacer do not exhibit an ordering exotherm on the first heating scan and therefore evidently order into a nematic mesophase from solution. Although this does not mean that the polymers are organized in solution, they at least order during precipitation due to the greater mobility of the longer spacer.

Figure 2 also presents the DSC traces of the polymers after annealing at room temperature for approximately 3 months. Compared to the reference polymers with a 1-carbon spacer, these polymers with an 11-carbon

Table 4. Thermal Transitions and Thermodynamic Parameters of Poly{5-[[[11′-[2″,5″-bis[2-(3′-fluoro-4′-*n*-alkoxyphenyl)ethynyl]phenyl]undecyl]oxy]carbonyl]-bicyclo[2.2.1]hept-2-ene}s[a]

			phase transitions, °C (ΔH, kJ/mru)	
n	DP$_\mathrm{n}$	% endo	heating	cooling
1	66	78	g 24 k 29 (0.47)	i 19 g
2	51	85	g 25 k 31 (1.58) n 48 (1.41) i	i 41 (1.19) n 20 g
3	36	73	g 29 k 35 (2.38) n 47 (0.88) i	i 38 (0.95) n 23 g
4	49	75	g 15 n 45 (1.27) i	i 39 (1.43) n 10 g
5	68	67	g 8 n 40 (1.38) i	i 35 (1.38) n 5 g
6	44	67	g 3 n 48 (2.08) i	i 44 (2.14) n −2 g
7	50	57	g 0 n 44 (1.86) i	i 40 (2.24) n −4 g
8	49	67	g −2 n 51 (2.69) i	i 47 (2.76) n −4 g
9	14	50	g −4 k 37 (15.7) n 41 (1.92) i	i 38 (1.73) n −9 g
9	17	50	g −3 k 40 (14.2) n 46 (1.47) i	i 43 (2.04) n −8 g
9	27	50	g −3 k 38 (1.53)[b] n 47 (1.43) i	i 44 (1.61) n −8 g
9	40	0	g −5 k 37 (3.11)[b] n 46 (2.11) i	i 42 (2.12) n −9 g
9	58	50	g −3 k 39 (16.5) n 48 (2.32) i	i 44 (2.58) n −7 g
9	91	50	g −3 k 37 (6.29)[b] n 49 (2.54) i	i 45 (2.91) n −7 g
9	158	50	g −3 k 38 (0.76) n 50 (2.19) i	i 46 (2.41) n −8 g
10	48	60	g −4 n 52 (3.10) i	i 49 (3.59) n −6 g
11	37	67	g −5 k 39 (11.1) n 50 (3.16) i	i 47 (3.16) n −7 g
12	45	67	g −3 n 53 (3.98) i	i 49 (4.23) n −9 g

[a] mru = mol repeat units; g = glass, k = crystalline, n = nematic, i = isotropic. [b] ΔH may be underestimated; annealed at room temperature for only 15−17 days.

spacer have much less tendency to crystallize. For example, the reference polymers with $n = 3-12$ crystallize after annealing at room temperature for only 1−2 weeks. In contrast, only a few of the polymers with the 11-carbon spacer ($n = 3, 9, 11$) crystallize after annealing at room temperature for 1 month. As shown by the annealed DSC scans in Figure 2, the $n = 1-2$ polymers also crystallize slightly after annealing at room temperature for 3 months. The greater ability of the reference polymers with the shorter 1-carbon spacer to crystallize compared to those with the longer 11-carbon spacer contrasts with the thermotropic behavior of SCLCPs with terminally attached mesogens. This indicates that it is the relatively rigid polynorbornene backbone that crystallizes rather than the mesogenic side chains.

Of the three polymers presented in Figure 2 that crystallize readily, two have the lowest molecular weights ($n = 3$, $\mathrm{DP_n} = 36$; $n = 11$, $\mathrm{DP_n} = 37$) and the third is based on the monomer with the lowest endo content ($n = 9$, 50% endo). We therefore explored the effect of both molecular weight ($\mathrm{DP_n} = 14-158$) and the isomeric content of the monomers (% exo = 50, 100) on the thermotropic behavior of the $n = 9$ polymer. Both Figure 2 and the data presented in Table 4 demonstrate that the $n = 9$ polymer with $\mathrm{DP_n} = 58$ crystallizes exceptionally well. It is almost completely crystallized after annealing at room temperature for 1−3 months; the glass transition is barely detectable, and the enthalpy of melting is quite large. In contrast to the $n = 3-12$ reference polymers which melt at a temperature just above their glass transitions, the $n = 9$ polymer with an 11-carbon spacer melts 41 °C above the glass transition, which is very close to the isotropization temperature. Therefore, crystallization is not impeded by the glass transition as it is in the reference polymers.

However, as with terminally attached SCLCPs,[20] the ability to crystallize decreases as the polymer's molecular weight increases since crystallization is kinetically controlled. As shown by the representative DSC heating scans in Figure 3 of the $n = 9$ polymers annealed at room temperature for 16−17 days, the lowest molecular weight polymers ($\mathrm{DP_n} = 14, 17$) crystallize to the greatest extent, whereas the highest molecular weight polymer ($\mathrm{DP_n} = 158$) does not crystallize at all after 17 days; however, it does crystallize slightly after 30 days. The polymers with intermediate molecular weights crystallize to intermediate extents. The polymer prepared from the 100% exo monomer also crystallizes, although it may not be quite as extensive as the polymers composed of only 50% of the exo isomer. However, the low endo isomeric content of the $n = 9$ polymer cannot explain its high crystallizability.

The phase transition temperatures of the $n = 9$ polymers observed on heating are plotted in Figure 4 as a function of the number-average degree of polymerization and $\mathrm{DP_n}^{-1}$. The transition temperatures reach a constant value at approximately 30 repeat units. This corresponds to $T_\mathrm{g} = -3$ °C, $T_\mathrm{m} = 38$ °C, and $T_\mathrm{i} = 50$ °C for an infinite molecular weight polymer according to extrapolation to $\mathrm{DP_n}^{-1} = 0$. The melting temperature does not vary with molecular weight, although an infinite molecular polymer should not be able to crystallize.

Figure 5 compares the phase diagram of the title polymers with an 11-carbon spacer and $\mathrm{DP_n} \geq 36$ to that of the 1,4-bis[(3′-fluoro-4′-*n*-alkoxyphenyl)ethynyl]-2-undecylbenzene model compounds. Figure 5 also compares the phase diagrams of the reference polymers with a 1-carbon spacer and their 1,4-bis[(3′-fluoro-4′-*n*-alkoxyphenyl)ethynyl]toluene model compounds. Although the nematic−isotropic transition temperatures of the reference polymers are depressed by 33−79 °C relative to their model compounds, the model compounds mimic both the nematic mesophase formed and the general decrease and specific variations in the isotropization temperature with increasing length of the *n*-alkoxy substituents. In addition, the reference polymers exhibit a crystalline phase over an extremely narrow temperature range when $n = 3-12$. In addition to the crystalline phase, their model compounds exhibit either a monotropic s_C mesophase or an enantiotropic s_C mesophase over a very narrow temperature range when $n = 9-12$.

Similarly, the 1,4-bis[(3′-fluoro-4′-*n*-alkoxyphenyl)-ethynyl]-2-undecylbenzene model compounds mimic both the nematic mesophase formed by the polymers with an 11-carbon spacer and the general invariance of their isotropization temperatures with increasing length of the *n*-alkoxy substituents. However, in this case, the glass transition temperatures of the polymers and the crystalline melting temperatures of the model compounds are significantly different relative to the isotropization temperatures. The nematic mesophase of the model compounds is monotropic when $n = 2, 4, 6-11$ and enantiotropic when $n = 12$; the model compounds with $n = 1, 3, 5$ do not exhibit a liquid-crystalline phase. All of the title polymers exhibit a nematic mesophase when $n > 1$. The nematic mesophase of all of the polymers with an 11-carbon spacer therefore occur over a much broader temperature range than that of their model compounds (Figure 5), except when the polymers crystallize and are therefore stabilized relative to the model compounds. The reference and title polymers exhibit the nematic mesophase over a similar temperature range. Therefore, increasing the spacer length from 1 to 11 carbons depresses the glass and isotropization transition temperatures to approximately the same extent. However, the crystalline melting transition of the lower molecular weight polymers is depressed less

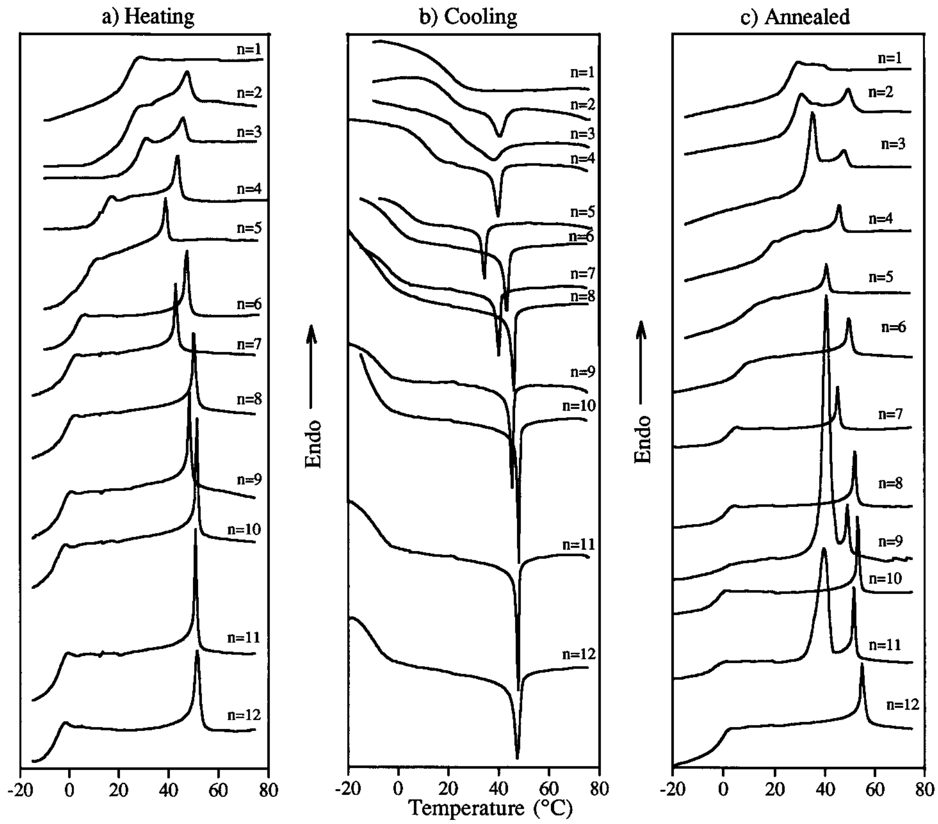

Figure 2. Normalized differential scanning calorimetry traces (10 °C/min) of poly{5-[[11′-[2″,5″-bis[2-[(3′-fluoro-4′-*n*-alkoxyphenyl)ethynyl]phenyl]undecyl]oxy]carbonyl]bicyclo[2.2.1]hept-2-ene}s: (a) heating scans of freshly precipitated polymers and of subsequent heating scans; (b) cooling scans; (c) heating scans of samples annealed at room temperature for approximately 3 months.

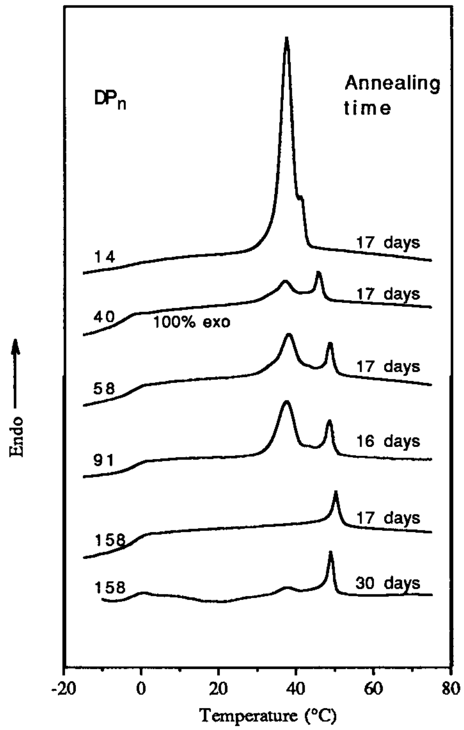

Figure 3. Normalized differential scanning calorimetry heating traces (10 °C/min) of poly{5-[[11′-[2″,5″-bis[2-[(3′-fluoro-4′-*n*-nonyloxyphenyl)ethynyl]phenyl]undecyl]oxy]carbonyl]bicyclo[2.2.1]hept-2-ene}s of varying chain lengths after annealing at room temperature for 17 days or longer.

than either isotropization or the glass transition by increasing spacer length, and the crystalline phase is therefore stabilized.

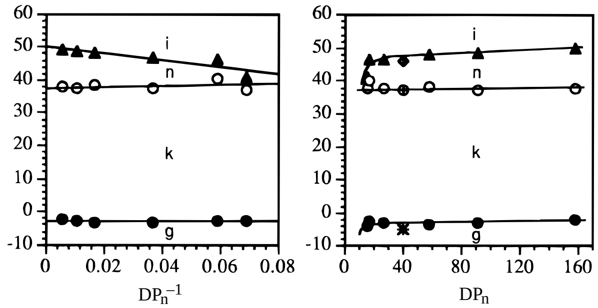

Figure 4. Dependence of the transition temperatures from the glass (●), crystalline (○), and nematic (▲) phases of poly{5-[[11′-[2″,5″-bis[2-[(3′-fluoro-4′-*n*-nonyloxyphenyl)ethynyl]phenyl]undecyl]oxy]carbonyl]bicyclo[2.2.1]hept-2-ene} as function of the GPC-determined number-average degree of polymerization and the inverse number-average degree of polymerization; all other symbols represent the corresponding transitions of the polymer based on the 100% exo monomer. Infinite molecular weight transitions: g −2.8 k 37.7 n 50.0 i.

Although the model compounds do not predict the temperature range over which the nematic mesophase of the polymers with an 11-carbon spacer is observed, their isotropization temperatures are nearly identical. This is surprising since the undecyl substituent of the model compounds and the 11-carbon spacer of the polymers should not have the same conformation relative to the mesogen. When the central ring of an extended mesogen is substituted laterally with a long *n*-alkyl or *n*-alkoxy group, the substituent lies parallel to the mesogen.[21] This enables the molecule to maintain a more rodlike shape and maximize packing. In contrast, the spacers are approximately perpendicular to the mesogens in laterally attached SCLCPs.[7]

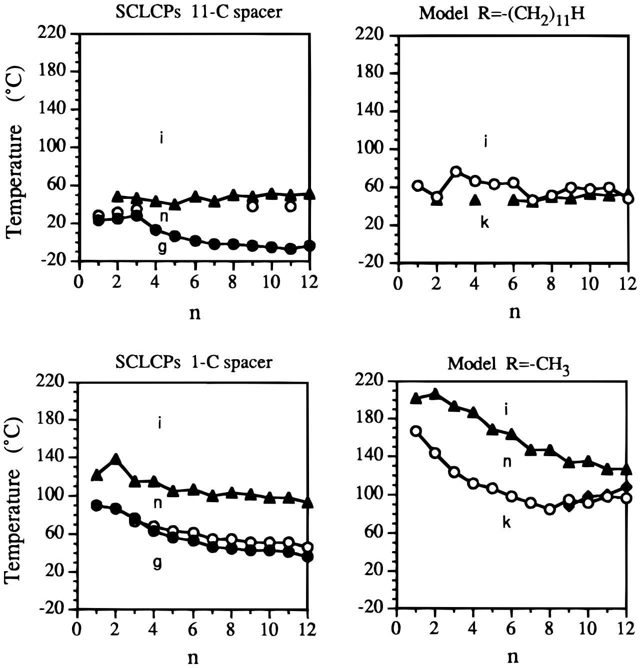

Figure 5. Transition temperatures of poly{5-[[11′-[2″,5″-bis-[2-[(3′-fluoro-4′-*n*-alkoxyphenyl)ethynyl]phenyl]undecyl]oxy]-carbonyl]bicyclo[2.2.1]hept-2-ene}s (SCLCPs 11-carbon spacer), {2,5-bis[(3′-fluoro-4′-*n*-alkoxyphenyl)ethynyl]phenyl}undecanes (model $-(CH_2)_{11}H$), poly{5-[[[2′,5′-bis[2-(3′-fluoro-4′-*n*-alkoxyphenyl)ethynyl]benzyl]oxy]carbonyl]bicyclo[2.2.1]hept-2-ene}s (SCLCPs 1-carbon spacer), and 2,5-bis[(3′-fluoro-4′-*n*-alkoxyphenyl)ethynyl]toluenes (model $-CH_3$) from the glassy (●), crystalline (○), smectic C (◆), and nematic (▲) states as a function of the length of the *n*-alkoxy substituents.

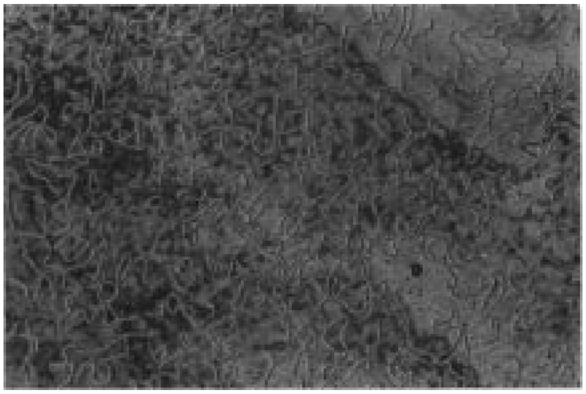

Figure 6. Polarized optical micrograph (200×) observed after annealing poly{5-[[11′-[2″,5″-bis[2-[(3′-fluoro-4′-*n*-heptoxyphenyl)ethynyl]phenyl]undecyl]oxy]carbonyl]bicyclo[2.2.1]hept-2-ene} at 43.2 °C for 16.5 h upon cooling from the isotropic melt; 43.2 °C, schlieren nematic texture.

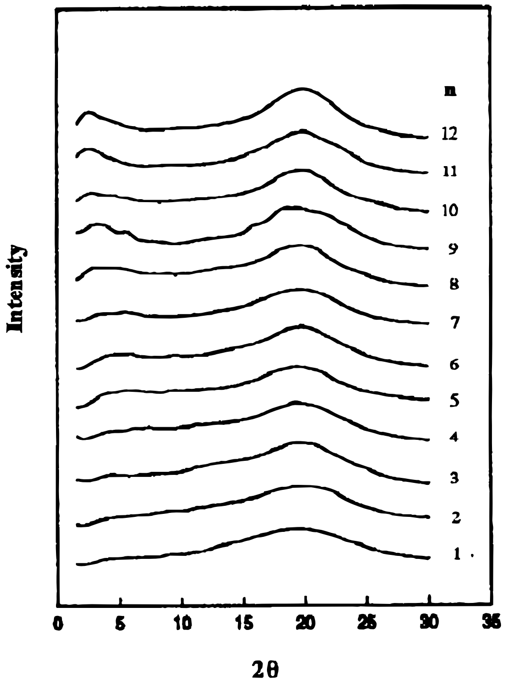

Figure 7. Wide-angle X-ray diffraction patterns of unoriented films of poly{5-[[11′-[2″,5″-bis[2-[(3′-fluoro-4′-*n*-alkoxyphenyl)-ethynyl]phenyl]undecyl]oxy]carbonyl]bicyclo[2.2.1]hept-2-ene}s recorded in the nematic phase at room temperature.

The nematic mesophase was difficult to identify by polarized optical microscopy. In contrast to the reference polymers, the polymers with an 11-carbon spacer do not form large nematic droplets upon cooling from the isotropic melt, even after extensive annealing in the biphasic region. As shown in Figure 6, the polarized optical micrographs of the polymers are highly threaded with bright wormlike defects in an otherwise homogeneous texture. However, the nematic mesophase was confirmed by wide-angle X-ray diffraction at room temperature. The powder WAXD patterns presented in Figure 7 of unoriented films exhibit only a diffuse diffraction at wide angles, which demonstrates that the mesogens are positionally disordered. Although a broad diffraction at low angle is starting to develop in those polymers with longer substituents, none of the polymers exhibit a sharp reflection at low angles that would correspond to the lamellar spacing of a smectic mesophase.

The fiber pattern of the $n = 2$ polymer is shown in Figure 8a. The nematic molecular arrangement is clearly identified by two pairs of diffuse scatterings along the equatorial direction and a pair of diffuse streaks on the meridian. The two pairs of diffuse scatterings along the equator correspond to disordered aliphatic distances from the spacers and intermolecular lateral packings within the molecular chains with *d* spacings of approximately 13.3 ($2\theta = 6.64°$) and 4.30 Å ($2\theta = 20.7°$), respectively. The diffuse streaks on the meridian correspond to the associated order from the mesogenic groups at 7.47 Å ($2\theta = 11.9°$) in an interdigitated arrangement. This fiber pattern is also representative of the X-ray fiber patterns of the $n = 1$ and $n = 3$ polymers, albeit with slightly different *d* spacings.

However, the fiber patterns of the polymers with $n \geq 4$ demonstrate that their molecular arrangement is different. The mesogens are again organized in a nematic mesophase. As shown by the representative fiber pattern of the $n = 5$ polymer in Figure 8b, the low ($2\theta = 6.91°$, 12.8 Å) and wide ($2\theta = 20.6°$, 4.30 Å) angle *d* spacings on the equator correspond to the disordered aliphatic spacer lengths and intermolecular lateral packings within the chains, respectively. However, the diffuse first-order diffraction from the mesogens at $2\theta = 5.90°$ on the meridian corresponds to a *d* spacing of 15.0 Å, which demonstrates that the mesogens tend to be aligned. Nevertheless, the diffraction is diffuse, which demonstrates that the correlation length along the lateral direction is poor. Therefore, although the mesogens of the polymers with $n \geq 4$ have some smectic alignment, we have assigned their arrangement to a nematic mesophase based on the poor correlation lengths along the lateral direction.

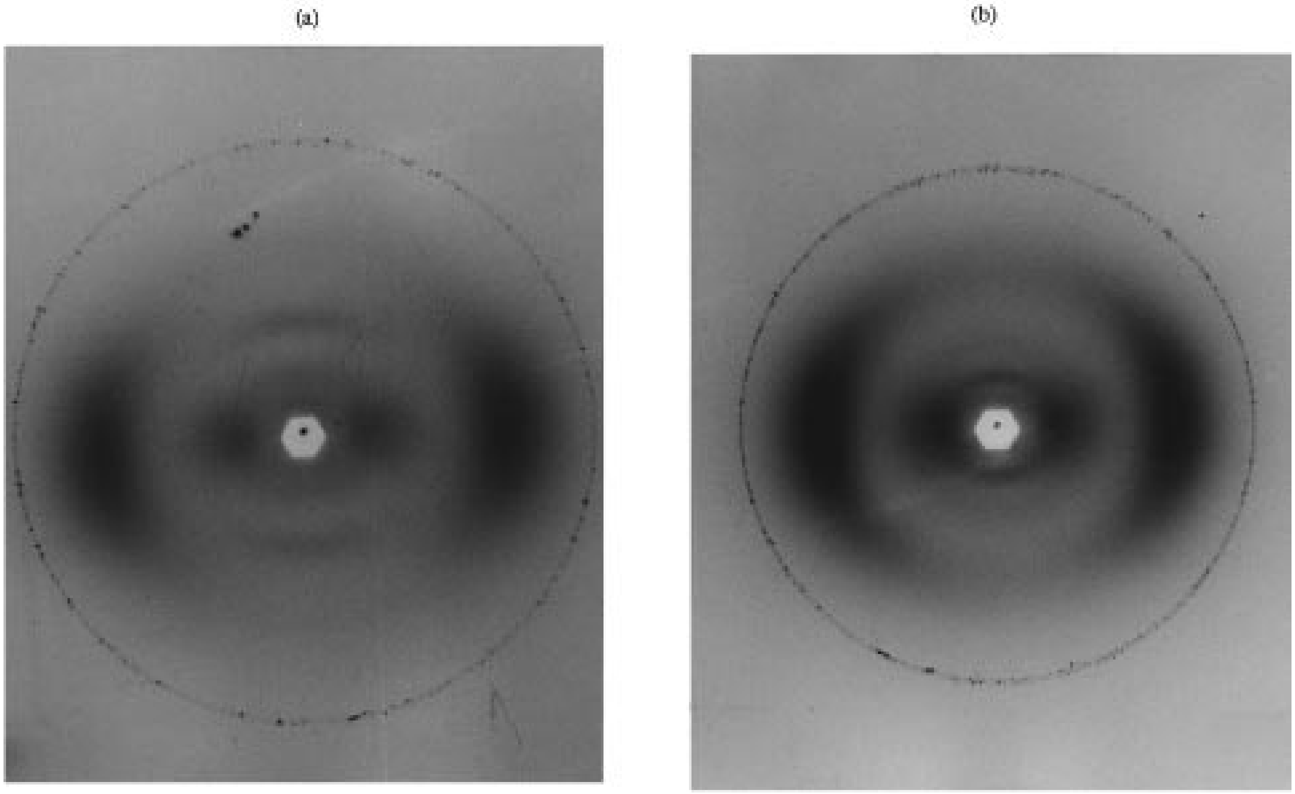

Figure 8. Wide-angle X-ray diffraction pattern of oriented fibers of poly{5-[[11′-[2″,5″-bis[2-[(3′-fluoro-4′-*n*-alkoxyphenyl)ethynyl]-phenyl]undecyl]oxy]carbonyl]bicyclo[2.2.1]hept-2-ene} recorded in the glassy state at room temperature: (a) $n = 2$; (b) $n = 5$.

In addition, the X-ray fiber pattern of the $n = 9$ polymer ($DP_n = 58$) confirmed that it crystallizes at room temperature after 7 days. The *d* spacings of the ordered crystalline phase at 15.0, 5.65, 4.98, 4.44, and 4.05 Å; are superimposed on the nematic organization. Our preliminary calculations indicate that this crystalline packing corresponds to a monoclinic unit cell. The detailed molecular packing will be described further in a future publication.

Conclusions

Since symmetrically disubstituted, extended mesogens tend to exhibit s_C mesophases, SCLCPs with laterally attached (vs terminally attached) mesogens offer an ideal architecture for obtaining s_C and s_C* mesophases. However, poly{5-[[[11′-[2″,5″-bis[2-(3′-fluoro-4′-*n*-alkoxyphenyl)ethynyl]phenyl]undecyl]oxy]-carbonyl]bicyclo[2.2.1]hept-2-ene}s exhibit only an enantiotropic nematic mesophase when $n = 2-12$, even though the corresponding 1,4-bis[(3′-fluoro-4′-*n*-alkoxyphenyl)ethynyl]benzenes exhibit a s_C-nematic phase sequence when $n = 6-12$. Both the nematic mesophase and the isotropization temperatures of these polymers are modeled more appropriately by 1,4-bis[(3′-fluoro-4′-*n*-alkoxyphenyl)ethynyl]-2-undecylbenzenes, which are based on the same mesogen, but are further substituted with an undecyl group to mimic the 11-carbon spacer of the polymer. Since even these polymers with an 11-carbon spacer do not exhibit a s_C mesophase, the mesogen density must be increased along the polynorbornene backbone in order to favor smectic mesophase formation.

Experimental Section

Materials. Acetyl chloride (Aldrich, 98%), bis(triphenylphosphine)palladium(II) chloride (Lancaster), borane–tetrahydrofuran (Aldrich, 1.0 M), cuprous iodide (Aldrich, 98%), (trimethylsilyl)acetylene (Lancaster, 98%), triphenylphosphine (Aldrich, 99%), 1-undecene (Fluka, 95%), and 10-undecenyl alcohol (Aldrich, 98%) were used as received. 1,4-Benzoquinone (Aldrich, 98%) was recrystallized from petroleum ether. Benzaldehyde (Aldrich, 99%) was distilled under N_2. Bicyclo[2.2.1]hept-2-ene-5-carboxyl chloride (78:22 = endo:exo) was synthesized as described previously.[10,22] The 1-bromo-3-fluoro-4-*n*-alkoxybenzenes ($n = 1-12$) were prepared in 64–99% yield by Williamson etherification of 4-bromo-2-fluorophenol (Aldrich, 98%) with either an *n*-bromoalkane or dimethyl or diethyl sulfate as described previously.[3,23] $Mo(CHCMe_2Ph)(N\text{-}2,6\text{-}{}^iPr_2Ph)(O^tBu)_2$ was synthesized by a literature procedure,[24] except that hexanes were used instead of pentane throughout the synthesis. Trifluoromethanesulfonic anhydride (triflic anhydride) was synthesized in 45–72% yield by dehydration of trifluoromethanesulfonic acid (Fisher, 98%).[18] Dimethylformamide was dried by distilling from CaH_2 under N_2. Pyridine (Fisher) and triethylamine (Lancaster) were distilled from KOH under nitrogen before use. Reagent-grade tetrahydrofuran (THF) was dried by distillation from purple sodium benzophenone ketyl under N_2. THF used as a polymerization solvent was vacuum transferred from purple sodium benzophenone ketyl on a high vacuum line and then vigorously degassed by several freeze–pump–thaw cycles immediately before use. All other reagents and solvents were commercially available and were used as received.

Techniques. All polymerizations were performed under a N_2 atmosphere in a Vacuum Atmospheres drybox. Unless noted otherwise, all other reactions were performed outside the drybox under a N_2 atmosphere using a Schlenk line. ^1H NMR spectra (δ, ppm) were recorded on either a Bruker AC-200 (200 MHz) or a Bruker AM-300 (300 MHz) spectrometer. Unless noted otherwise, all spectra were recorded in $CDCl_3$ with TMS as an internal standard. Relative molecular weights were determined by gel permeation chromatography (GPC) at 35 °C using THF as solvent (1.0 mL/min), a set of 50, 100, 500, and 10^4 Å and linear ($50-10^4$ Å) Styragel 5 μm columns, a Waters 486 tunable UV/vis detector set at 290 nm, and a Waters 410 differential refractometer.

The thermotropic behavior of all compounds was determined by a combination of differential scanning calorimetry (DSC) and polarized optical microscopy. A Perkin-Elmer DSC-7 differential scanning calorimeter was used to determine the thermal transitions at 10 °C/min. The endothermic and exothermic peaks were read at their maximum and minimum energies, respectively. Glass transition temperatures (T_gs) were read as the middle of the change in heat capacity. All of the samples were initially heated three times and cooled twice; their equilibrium transition temperatures and enthalpies were subsequently determined through extensive annealing and quenching studies. Both enthalpy changes and transition temperatures were determined using indium and zinc as calibration standards. A Leitz Laborlux 12 Pol S polarized optical microscope (magnification 200×) equipped with a Mettler FP82 hot stage and a Mettler FP90 central processor was used to observe the thermal transitions and to analyze the anisotropic textures.[19] Thin samples were prepared either by capillary flow or by melting a minimum amount of compound between a clean glass slide and a cover slip and rubbing the cover slip with a spatula.

Wide-angle X-ray diffraction (WAXD) experiments were carried out on a Rigaku 12 kW rotating-anode generator (Rotaflex RU-200BH) at room temperature (50 kV and 150 mA). All of the powder samples were measured in the transmission mode. The Ni-filtered Cu Kα radiation was monochromatized using a graphite crystal. A diffractometer was coupled with the generator and a scanning 2θ angle range was between 1.5° and 30° at a scanning rate of 3°/min. The background air scattering was subtracted from each sample measurement using a blank scan. Fiber samples with a diameter of approximately 50 μm were prepared by melt spinning. The as-spun fibers were mounted in a vacuum flat camera which was coupled with a Rigaku tube X-ray generator (40 kV and 30 mA). The same Cu Kα radiation was used. Silicon powders with known crystal sizes were used in a 2θ angle calibration (28.46°). The exposure time was 24 h.

Synthesis of Monomers and Precursors. 10-Undecenyl Acetate. Acetyl chloride (47 g, 0.60 mol) was added dropwise over 1.5 h to an ice-cooled solution of 10-undecenyl alcohol (95 g, 0.56 mol) and triethylamine (71 g, 0.70 mol) in dry THF (100 mL). The reaction mixture was stirred at room temperature for 10 h and then poured into water (500 mL). This was extracted with Et$_2$O, and the Et$_2$O extracts were washed sequentially with water, aqueous NaHCO$_3$, and water. After the organic extracts were dried over MgSO$_4$, the solution was filtered and the solvent was removed by rotary evaporation. The residue was distilled (102−105 °C/1 mmHg) to yield 110 g (93%) of 10-undecenyl acetate as a clear, colorless oil. ^{1}H NMR: 1.27 (m, $-[\mathrm{C}H_2]_6-$), 1.58 (m, $-\mathrm{C}H_2\mathrm{CH_2OAc}$), 2.02 (m, $-\mathrm{C}H_2\mathrm{CH}=$), 2.05 (s, $\mathrm{C}H_3\mathrm{CO_2}-$), 4.04 (t, $-\mathrm{C}H_2\mathrm{OAc}$), 4.94 (m, $=\mathrm{C}H_2$), 5.81 (m, $=\mathrm{C}H-$).

2-Undecyl-1,4-hydroquinone. 2-Undecyl-1,4-hydroquinone was synthesized in 81−90% yield as in the following example. A 1.0 M borane solution in THF (52 mL, 52 mmol) was added dropwise to ice-cooled 1-undecene (23 g, 0.15 mol). The reaction mixture was stirred at 0 °C until ^{1}H NMR demonstrated that the vinyl groups were completely consumed by hydroboration (2 h). A solution of 1,4-benzoquinone (5.4 g, 50 mmol) in dry THF (40 mL) was then added all at once, and the mixture was stirred at 0 °C for 15 min and then at room temperature for 2 h. Water (5 mL) was added to this mixture, and it was stirred overnight. The reaction mixture was poured into a saturated aqueous solution of NaCl and extracted three times with Et$_2$O (80 mL each). The Et$_2$O extracts were washed sequentially with saturated NaCl and 10% aqueous NaHCO$_3$. After the organic extracts were dried over MgSO$_4$, the solution was filtered and the solvent was removed by rotary evaporation. The residue was recrystallized twice from Et$_2$O/hexanes (3:7) to yield 11 g (86%) of 2-undecyl-1,4-hydroquinone as white crystals; mp 76−78 °C. ^{1}H NMR: 0.88 (t, $-\mathrm{C}H_3$), 1.26 (m, $-[\mathrm{C}H_2]_8-$), 1.56 (m, $-\mathrm{C}H_2\mathrm{CH_2Ar}$), 2.54 (t, $-\mathrm{C}H_2\mathrm{Ar}$), 4.39 (s, $-\mathrm{O}H$), 4.44 (s, $-\mathrm{O}H$), 6.54 (dd, 1 aromatic H para to $-\mathrm{CH_2}-$), 6.62 (d, 1 aromatic H ortho $-\mathrm{CH_2}-$), 6.64 (d, 1 aromatic H meta to $-\mathrm{CH_2}-$).

11-(2′,5′-Dihydroxyphenyl)undecyl Acetate. Starting with 10-undecenyl acetate, 11-(2′,5′-dihydroxyphenyl)undecyl acetate was prepared in 76−82% yield by the same procedure described above to synthesize 2-undecyl-1,4-hydroquinone; mp 100−102 °C, white crystals. ^{1}H NMR: 1.27 (m, $-[\mathrm{C}H_2]_7-$), 1.59 (m, $-\mathrm{C}H_2\mathrm{CH_2OAc}$ and $-\mathrm{C}H_2\mathrm{CH_2Ar}$), 2.05 (s, $\mathrm{C}H_3\mathrm{CO_2}-$), 2.54 (t, $-\mathrm{C}H_2\mathrm{Ar}$), 4.06 (t, $-\mathrm{C}H_2\mathrm{OAc}$), 4.44 (s, $-\mathrm{O}H$), 4.54 (s, $-\mathrm{O}H$), 6.54 (dd, 1 aromatic H para to $-\mathrm{CH_2}-$), 6.62 (d, 1 aromatic H ortho to $-\mathrm{CH_2}-$), 6.64 (d, 1 aromatic H meta to $-\mathrm{CH_2}-$).

{2,5-Bis[[(trifluoromethyl)sulfonyl]oxy]phenyl}undecane. {2,5-Bis[[(trifluoromethyl)sulfonyl]oxy]phenyl}undecane was prepared in 56−76% yield using the following procedure. Trifluoromethanesulfonic anhydride (20 g, 70 mmol) was added dropwise to an ice-cooled solution of 2-undecyl-1,4-hydroquinone (8.5 g, 32 mmol) in dry pyridine (20 mL), and the reaction mixture was stirred at room temperature for 25 h. The reaction mixture was poured into water and extracted three times with Et$_2$O (60 mL each). The Et$_2$O extracts were washed sequentially with aqueous NaCl, 5% HCl, concentrated aqueous NaHCO$_3$, and water. After the organic extracts were dried over MgSO$_4$, the solution was filtered and the solvent was removed by rotary evaporation. The residue was purified by column chromatography using silica gel as the stationary phase and Et$_2$O/hexanes (2:8) as the eluant. The solvent was removed in vacuo to yield 13 g (75%) of {2,5-bis[[(trifluoromethyl)sulfonyl]oxy]phenyl}undecane as a colorless oil. ^{1}H NMR: 0.88 (t, $-\mathrm{C}H_3$), 1.27 (m, $-[\mathrm{C}H_2]_8-$), 1.64 (m, $-\mathrm{C}H_2\mathrm{CH_2Ar}$), 2.73 (t, $-\mathrm{C}H_2\mathrm{Ar}$), 7.21 (dd, 1 aromatic H para to $-\mathrm{CH_2}-$), 7.25 (d, 1 aromatic H ortho to $-\mathrm{CH_2}-$), 7.35 (d, 1 aromatic H meta to $-\mathrm{CH_2}-$).

11-{2′,5′-Bis[[(trifluoromethyl)sulfonyl]oxy]phenyl}undecyl Acetate. Starting with 11-(2′,5′-dihydroxyphenyl)undecyl acetate, 11-{2′,5′-bis[[(trifluoromethyl)sulfonyl]oxy]phenyl}undecyl acetate was prepared in 70−87% yield by the same procedure described above to synthesize {2,5-bis[[(trifluoromethyl)sulfonyl]oxy]phenyl}undecane; colorless oil. ^{1}H NMR: 1.28 (m, $-[\mathrm{C}H_2]_7-$), 1.60 (m, $-\mathrm{C}H_2\mathrm{CH_2OAc}$ and $-\mathrm{C}H_2\mathrm{CH_2Ar}$), 2.04 (s, $\mathrm{C}H_3\mathrm{CO_2}-$), 2.72 (t, $-\mathrm{C}H_2\mathrm{Ar}$), 4.05 (t, $-\mathrm{C}H_2\mathrm{OAc}$), 7.19 (dd, 1 aromatic H para to $-\mathrm{CH_2}-$), 7.24 (d, 1 aromatic H ortho to $-\mathrm{CH_2}-$), 7.34 (d, 1 aromatic H meta to $-\mathrm{CH_2}-$).

{2,5-Bis[2′-(trimethylsilyl)acetylene]phenyl}undecane. {2,5-Bis[2′-(trimethylsilyl)acetylene]phenyl}undecane was prepared in 61−81% yield. In a typical example, a solution of {2,5-bis[[(trifluoromethyl)sulfonyl]oxy]phenyl}undecane (10 g, 19 mmol), (trimethylsilyl)acetylene (4.4 g, 45 mmol), and triethylamine (5.1 g, 50 mmol) in dry DMF (50 mL) was added all at once to a mixture of PdCl$_2$(PPh$_3$)$_2$ (1.4 g, 2.0 mmol), triphenylphosphine (2.6 g, 10 mmol), and CuI (1.5 g, 8.0 mmol), and the reaction mixture was stirred at 90 °C for 25 h. It was then cooled to room temperature and poured into a saturated aqueous solution of NH$_4$Cl (200 mL), and the resulting mixture was extracted three times with Et$_2$O (80 mL each). The Et$_2$O extracts were washed sequentially with water, 5% aqueous HCl, and water and then dried over MgSO$_4$. After filtration and removal of the solvent on a rotary evaporator, the resulting liquid was purified by column chromatography using silica gel as the stationary phase and Et$_2$O/hexanes (1:9) as the eluant. The solvent was removed in vacuo to yield 5.8 g (72%) of {2,5-bis[2′-(trimethylsilyl)acetylene]phenyl}undecane as a clear, slightly yellow oil. ^{1}H NMR: 0.24 (s, $-\mathrm{Si(C}H_3)_3$, 18 H), 0.88 (t, $-\mathrm{C}H_3$), 1.26 (m, $-[\mathrm{C}H_2]_8-$), 1.61 (m, $-\mathrm{C}H_2\mathrm{CH_2Ar}$), 2.72 (t, $-\mathrm{C}H_2\mathrm{Ar}$), 7.21 (dd, 1 aromatic H para to $-\mathrm{CH_2}-$), 7.28 (d, 1 aromatic H ortho to $-\mathrm{CH_2}-$), 7.34 (d, 1 aromatic H meta to $-\mathrm{CH_2}-$).

11-{2′,5′-Bis[2″-(trimethylsilyl)acetylene]phenyl}undecyl Acetate. Starting with 11-{2′,5′-bis[[(trifluoromethyl)sulfonyl]oxy]phenyl}undecyl acetate, 11-{2′,5′-bis[2″-(trimethylsilyl)acetylene]phenyl}undecyl acetate was prepared in 71−86% yield by the same procedure described above to synthesize {2,5-bis[2′-(trimethylsilyl)acetylene]phenyl}undecane; slightly yellow oil. ^{1}H NMR: 0.23 (s, $-\mathrm{Si(C}H_3)_3$, 18 H), 1.27 (m, $-[\mathrm{C}H_2]_7-$), 1.60 (m, $-\mathrm{C}H_2\mathrm{CH_2OAc}$ and $-\mathrm{C}H_2\mathrm{CH_2Ar}$), 2.04 (s, $\mathrm{C}H_3\mathrm{CO_2}-$), 2.71 (t, $-\mathrm{C}H_2\mathrm{Ar}$), 4.05 (t, $-\mathrm{C}H_2\mathrm{OAc}$), 7.21 (dd, 1 aromatic H para to $-CH_2-$), 7.28 (d, 1 aromatic H ortho to $-CH_2-$), 7.34 (d, 1 aromatic H meta to $-CH_2-$).

[2,5-Bis(acetylene)phenyl]undecane. [2,5-Bis(acetylene)phenyl]undecane was prepared in 85−95% yield using the following procedure. A mixture of {2,5-bis[2′-(trimethylsilyl)acetylene]phenyl}undecane (5.5 g, 13 mmol) and K_2CO_3 (5.5 g, 40 mmol) in methanol (40 mL) was stirred at room temperature for 10 h. It was then poured into water and extracted three times with Et_2O (60 mL each). The Et_2O extracts were dried over $MgSO_4$, filtered, and concentrated on a rotary evaporator. The resulting liquid was purified by column chromatography using silica gel as the stationary phase and Et_2O/hexanes (1:9) as the eluant. The solvent was removed in vacuo to yield 3.5 g (95%) of [2,5-bis(acetylene)phenyl]undecane as a clear, slightly yellow oil. ^1H NMR: 0.88 (t, $-CH_3$), 1.26 (m, $-[CH_2]_8-$), 1.62 (m, $-CH_2CH_2Ar$), 2.75 (t, $-CH_2Ar$), 3.13 (s, $HC\equiv$), 3.31 (s, $HC\equiv$), 7.26 (dd, 1 aromatic H para to $-CH_2-$), 7.33 (d, 1 aromatic H ortho to $-CH_2-$), 7.41 (d, 1 aromatic H meta to $-CH_2-$).

11-[2′,5′-Bis(acetylene)phenyl]undecanol. 11-[2′,5′-Bis(acetylene)phenyl]undecanol was prepared in 88−96% yield. In a typical example, a mixture of 11-{2′,5′-bis[2″-(trimethylsilyl)acetylene]phenyl}undecyl acetate (8.0 g, 17 mmol) and K_2CO_3 (8.3 g, 80 mmol) in methanol (40 mL) was stirred at room temperature for 12 h and at 50 °C for 0.5 h. The reaction mixture was concentrated on a rotary evaporator, and the residue was extracted three times with Et_2O (60 mL each). The Et_2O extracts were washed sequentially with water, dilute aqueous HCl, and water and were dried over $MgSO_4$. After filtration and removal of the solvent on a rotary evaporator, the resulting liquid was purified by column chromatography using silica gel as the stationary phase and Et_2O/hexanes (1:2) as the eluant. The solvent was removed in vacuo to yield 4.7 g (96%) of 11-[2′,5′-bis(acetylene)phenyl]undecanol as a slightly yellow oil. ^1H NMR: 1.26 (m, $-[CH_2]_7-$), 1.58 (m, $-CH_2CH_2OAc$ and $-CH_2CH_2Ar$), 2.75 (t, $-CH_2Ar$), 3.14 (s, $HC\equiv$), 3.32 (s, $HC\equiv$), 3.64 (t, $-CH_2OH$), 7.26 (dd, 1 aromatic H para to $-CH_2-$), 7.32 (d, 1 aromatic H ortho to $-CH_2-$), 7.40 (d, 1 aromatic H meta to $-CH_2-$).

{2,5-Bis[(3′-fluoro-4′-*n*-alkoxyphenyl)ethynyl]phenyl}undecanes (*n* = 1−12). The {2,5-bis[(3′-fluoro-4′-*n*-alkoxyphenyl)ethynyl]phenyl}undecanes were prepared in 33−50% yield as in the following example. A solution of 2,5-[bis(acetylene)phenyl]undecane (0.28 g, 1.0 mmol), 1-bromo-3-fluoro-(4-methoxy)benzene (0.51 g, 2.5 mmol), and triethylamine (0.35 g, 3.5 mmol) in dry THF (30 mL) was added all at once to a mixture of $PdCl_2(PPh_3)_2$ (70 mg, 0.10 mmol), triphenylphosphine (0.13 g, 0.50 mmol), and CuI (76 mg, 0.40 mmol), and the reaction mixture was stirred at reflux for 22 h. It was then cooled to room temperature and poured into a saturated aqueous solution of NH_4Cl (100 mL), and the resulting mixture was extracted three times with Et_2O (50 mL each). The Et_2O extracts were washed sequentially with water, 5% aqueous HCl, and water and then dried over $MgSO_4$. After filtration and removal of the solvent on a rotary evaporator, the resulting dark brown liquid was purified by column chromatography using silica gel as the stationary phase and hexanes/ether (9:1) as the eluant. The resulting slightly yellow solid (0.35 g, 65% crude yield) was recrystallized from Et_2O/methanol (4:5) to yield 0.26 g (50%) of {2,5-bis[(3′-fluoro-4′-methoxyphenyl)ethynyl]phenyl}undecane as white crystals. ^1H NMR: 0.87 (t, $-CH_3$), 1.25 (m, $-[CH_2]_8-$), 1.70 (m, $-CH_2CH_2Ar$), 2.81 (t, $-CH_2Ar$), 3.92 (s, $-OCH_3$, 6 H), 6.93 (ddd, 2 aromatic H ortho to $-OCH_3$), 7.26 (m, 4 aromatic H meta to $-OCH_3$), 7.30 (dd, 1 aromatic H para to $-CH_2-$), 7.37 (d, 1 aromatic H ortho to $-CH_2-$), 7.44 (d, 1 aromatic H meta to $-CH_2-$). Anal. ($C_{35}H_{38}F_2O_2$) C, H: calcd, 79.52, 7.24; found, 79.78, 7.46.

{2,5-Bis[(3′-fluoro-4′-ethoxyphenyl)ethynyl]phenyl}undecane. ^1H NMR: 0.87 (t, $-CH_3$), 1.24 (m, $-[CH_2]_8-$), 1.47 (t, CH_3CH_2O-, 6 H), 1.69 (m, $-CH_2CH_2Ar$), 2.81 (t, $-CH_2Ar$), 4.14 (q, $-OCH_2-$, 4 H), 6.92 (ddd, 2 aromatic H ortho to $-OCH_2-$), 7.24 (m, 4 aromatic H meta to $-OCH_2-$), 7.30 (dd, 1 aromatic H para to $-CH_2-$), 7.36 (d, 1 aromatic H ortho to $-CH_2-$), 7.43 (d, 1 aromatic H meta to $-CH_2-$). Anal. ($C_{37}H_{42}F_2O_2$) C, H: calcd, 79.82, 7.60; found, 80.46, 7.81.

{2,5-Bis[(3′-fluoro-4′-*n*-propoxyphenyl)ethynyl]phenyl}undecane. ^1H NMR: 0.87 (t, $-CH_3$), 1.06 (t, $CH_3[CH_2]_2O-$, 6 H), 1.24 (m, $-[CH_2]_8-$), 1.69 (m, $-CH_2CH_2Ar$), 1.86 (m, $-CH_2CH_2O-$, 4 H), 2.81 (t, $-CH_2Ar$), 4.02 (t, $-OCH_2-$, 4 H), 6.92 (ddd, 2 aromatic H ortho to $-OCH_2-$), 7.24 (m, 4 aromatic H meta to $-OCH_2-$), 7.30 (dd, 1 aromatic H para to $-CH_2-$), 7.36 (d, 1 aromatic H ortho to $-CH_2-$), 7.43 (d, 1 aromatic H meta to $-CH_2-$). Anal. ($C_{39}H_{46}F_2O_2$) C, H: calcd, 80.10, 7.94; found, 80.42, 8.09.

{2,5-Bis[(3′-fluoro-4′-*n*-butoxyphenyl)ethynyl]phenyl}undecane. ^1H NMR: 0.87 (t, $-CH_3$), 0.99 (t, $CH_3[CH_2]_3O-$, 6 H), 1.25 (m, $-[CH_2]_8-$), 1.52 (m, $-CH_2[CH_2]_2O-$, 4 H), 1.69 (m, $-CH_2CH_2Ar$), 1.82 (m, $-CH_2CH_2O-$, 4 H), 2.81 (t, $-CH_2Ar$), 4.06 (t, $-OCH_2-$, 4 H), 6.92 (ddd, 2 aromatic H ortho to $-OCH_2-$), 7.23 (m, 4 aromatic H meta to $-OCH_2-$), 7.30 (dd, 1 aromatic H para to $-CH_2-$), 7.36 (d, 1 aromatic H ortho to $-CH_2-$), 7.43 (d, 1 aromatic H meta to $-CH_2-$). Anal. ($C_{41}H_{50}F_2O_2$) C, H: calcd, 80.36, 8.22; found, 79.38, 8.38.

{2,5-Bis[(3′-fluoro-4′-*n*-pentoxyphenyl)ethynyl]phenyl}undecane. ^1H NMR: 0.87 (t, $-CH_3$), 0.94 (t, $CH_3[CH_2]_4O-$, 6 H), 1.15−1.55 (m, $-[CH_2]_8-$ and $-[CH_2]_2CH_2CH_2O-$, 24 H), 1.69 (m, $-CH_2CH_2Ar$), 1.84 (m, $-CH_2CH_2O-$, 4 H), 2.81 (t, $-CH_2Ar$), 4.05 (t, $-OCH_2-$, 4 H), 6.91 (ddd, 2 aromatic H ortho to $-OCH_2-$), 7.25 (m, 4 aromatic H meta to $-OCH_2-$), 7.30 (dd, 1 aromatic H para to $-CH_2-$), 7.36 (d, 1 aromatic H ortho to $-CH_2-$), 7.43 (d, 1 aromatic H meta to $-CH_2-$). Anal. ($C_{43}H_{54}F_2O_2$) C, H: calcd, 80.59, 8.49; found, 80.94, 8.76.

The ^1H NMR spectra of the {2,5-bis[(3′-fluoro-4′-*n*-alkoxyoxyphenyl)ethynyl]phenyl}undecanes with $n = 6-12$ are identical: 0.89 (t, $-CH_3$, 9 H), 1.15−1.60 (m, $-[CH_2]_8-$ and $-[CH_2]_{n-3}CH_2CH_2O-$, $4n + 4$ H), 1.69 (m, $-CH_2CH_2Ar$), 1.83 (m, $-CH_2CH_2O-$, 4 H), 2.81 (t, $-CH_2Ar$), 4.05 (t, $-OCH_2-$, 4 H), 6.91 (ddd, 2 aromatic H ortho to $-OCH_2-$), 7.23 (m, 4 aromatic H meta to $-OCH_2-$), 7.29 (dd, 1 aromatic H para to $-CH_2-$), 7.36 (d, 1 aromatic H ortho to $-CH_2-$), 7.43 (d, 1 aromatic H meta to $-CH_2-$). Anal. ($C_{45}H_{58}F_2O_2$) C, H: calcd, 80.80, 8.74; found, 81.03, 8.92. Anal. ($C_{47}H_{62}F_2O_2$) C, H: calcd, 80.99, 8.97; found, 80.95, 9.02. Anal. ($C_{49}H_{66}F_2O_2$) C, H: calcd, 81.17, 9.17; found, 81.32, 9.20. Anal. ($C_{51}H_{70}F_2O_2$) C, H: calcd, 81.34, 9.37; found, 81.60, 9.46. Anal. ($C_{53}H_{74}F_2O_2$) C, H: calcd, 81.49, 9.55; found, 81.67, 9.42. Anal. ($C_{55}H_{78}F_2O_2$) C, H: calcd, 81.63, 9.72; found, 81.60, 9.76. Anal. ($C_{57}H_{82}F_2O_2$) C, H: calcd, 81.77, 9.87; found, 81.96, 9.95.

11-{2′,5′-Bis[2-(3″-fluoro-4″-*n*-alkoxyphenyl)ethynyl]phenyl}undecanols (*n* = 1−12). The 11-{2′,5′-bis[2-(3″-fluoro-4″-*n*-alkoxyphenyl)ethynyl]phenyl}undecanols were synthesized in 30−50% yield as in the following example. A solution of 11-[2′,5′-bis(acetylene)phenyl]undecanol (1.2 g, 4.0 mmol), 1-bromo-3-fluoro-4-methoxybenzene (1.7 g, 8.5 mmol), and triethylamine (1.0 g, 10 mmol) in dry THF (15 mL) and DMF (5 mL) was added all at once to a mixture of $PdCl_2(PPh_3)_2$ (0.25 g, 0.36 mmol), triphenylphosphine (0.47 g, 1.8 mmol), and CuI (0.27 g, 1.4 mmol), and the reaction mixture was stirred at reflux for 38 h. It was then cooled to room temperature and poured into a saturated aqueous solution of NH_4Cl (200 mL), and the resulting mixture was extracted three times with Et_2O (50 mL each). The Et_2O extracts were washed sequentially with water, 5% aqueous HCl, and water and then dried over $MgSO_4$. After filtration and removal of the solvent on a rotary evaporator, the resulting dark liquid was purified by column chromatography using silica gel as the stationary phase and Et_2O/hexanes (2:8) as the eluant. The solvent was removed in vacuo, and the resulting oil was recrystallized twice from hexanes to yield 0.91 g (42%) of 11-{2′,5′-bis[2-(3″-fluoro-4″-methoxyphenyl)ethynyl]phenyl}undecanol as white crystals. ^1H NMR: 1.27 (m, $-[CH_2]_7-$), 1.55 (m, $-CH_2CH_2OH$), 1.70 (m, $-CH_2CH_2Ar$), 2.81 (t, $-CH_2Ar$), 3.63 (q, $-CH_2OH$), 3.92 (s, $-OCH_3$, 6 H), 6.93 (ddd, 2 aromatic H ortho to $-OCH_3$), 7.24 (m, 4 aromatic H meta to $-OCH_3$), 7.30 (dd, 1 aromatic H para to $-CH_2-$), 7.37 (d, 1 aromatic H ortho to $-CH_2-$), 7.44 (d, 1 aromatic H meta to $-CH_2-$).

11-{2′,5′-Bis[2-(3″-fluoro-4″-ethoxyphenyl)ethynyl]phenyl}undecanol. ^{1}H NMR: 1.27 (m, $-[CH_2]_7-$), 1.50 (t, $-CH_3$, 6 H), 1.55 (m, $-CH_2CH_2OH$, 4 H), 1.69 (m, $-CH_2CH_2Ar$), 2.81 (t, $-CH_2Ar$), 3.65 (q, $-CH_2OH$), 4.14 (q, $-CH_2OAr$, 4 H), 6.92 (ddd, 2 aromatic H ortho to $-OCH_2-$), 7.24 (m, 4 aromatic H meta to $-OCH_2-$), 7.30 (dd, 1 aromatic H para to $-CH_2-$), 7.36 (d, 1 aromatic H ortho to $-CH_2-$), 7.43 (d, 1 aromatic H meta to $-CH_2-$).

11-{2′,5′-Bis[2-(3″-fluoro-4″-*n*-propoxyphenyl)ethynyl]phenyl}undecanol. ^{1}H NMR: 1.06 (t, $-CH_3$, 6 H), 1.27 (m, $-[CH_2]_7-$), 1.55 (m, $-CH_2CH_2OH$, 4 H), 1.69 (m, $-CH_2CH_2Ar$), 1.86 (m, $-CH_2CH_2OAr$, 4 H), 2.81 (t, $-CH_2Ar$), 3.63 (q, $-CH_2OH$), 4.02 (t, $-CH_2OAr$, 4 H), 6.93 (ddd, 2 aromatic H ortho to $-OCH_2-$), 7.23 (m, 4 aromatic H meta to $-OCH_2-$), 7.30 (dd, 1 aromatic H para to $-CH_2-$), 7.36 (d, 1 aromatic H ortho to $-CH_2-$), 7.43 (d, 1 aromatic H meta to $-CH_2-$).

11-{2′,5′-Bis[2-(3″-fluoro-4″-*n*-butoxyphenyl)ethynyl]phenyl}undecanol. ^{1}H NMR: 0.99 (t, $-CH_3$, 6 H), 1.27 (m, $-[CH_2]_7-$), 1.55 (m, $-CH_2CH_2OH$ and $-CH_2[CH_2]_2O-$, 6 H), 1.69 (m, $-CH_2CH_2Ar$), 1.82 (m, $-CH_2CH_2OAr$, 4 H), 2.81 (t, $-CH_2Ar$), 3.63 (q, $-CH_2OH$), 4.06 (t, $-CH_2OAr$, 4 H), 6.92 (ddd, 2 aromatic H ortho to $-OCH_2-$), 7.24 (m, 4 aromatic H meta to $-OCH_2-$), 7.29 (dd, 1 aromatic H para to $-CH_2-$), 7.36 (d, 1 aromatic H ortho to $-CH_2-$), 7.43 (d, 1 aromatic H meta to $-CH_2-$).

The ^{1}H NMR spectra of the 11-{2′,5′-bis[2-(3″-fluoro-4″-*n*-alkoxyphenyl)ethynyl]phenyl}undecanols with $n = 5-12$ are identical: 0.90 (t, $-CH_3$, 6 H), 1.15−1.60 (m, $-[CH_2]_8-$ and $-[CH_2]_{n-3}CH_2CH_2O-$, $4n + 4$ H), 1.69 (m, $-CH_2CH_2Ar$), 1.83 (m, $-CH_2CH_2OAr$, 4 H), 2.81 (t, $-CH_2Ar$), 3.63 (q, $-CH_2OH$), 4.05 (t, $-CH_2OAr$, 4 H), 6.92 (ddd, 2 aromatic H ortho to $-OCH_2-$), 7.23 (m, 4 aromatic H meta to $-OCH_2-$), 7.30 (dd, 1 aromatic H para to $-CH_2-$), 7.36 (d, 1 aromatic H ortho to $-CH_2-$), 7.43 (d, 1 aromatic H meta to $-CH_2-$).

5-{[[11′-[2″,5″-Bis[2-(3′-fluoro-4′-*n*-alkoxyphenyl)ethynyl]phenyl]undecyl]oxy]carbonyl}bicyclo[2.2.1]hept-2-enes ($n = 1-12$, 50−85% endo). The 5-{[[11′-[2″,5″-bis[2-(3′-fluoro-4′-*n*-alkoxyphenyl)ethynyl]phenyl]undecyl]oxy]carbonyl}bicyclo[2.2.1]hept-2-enes were prepared in 75−97% yield as in the following example. A solution of bicyclo[2.2.1]hept-2-ene-5-carboxyl chloride (0.31 g, 2.0 mmol) in dry THF (5 mL) was added dropwise to an ice-cooled solution of 11-{2′,5′-bis[2-(3″-fluoro-4″-methoxyphenyl)ethynyl]phenyl}undecanol (0.90 g, 1.6 mmol) and triethylamine (0.25 g, 2.5 mmol) in dry THF (5 mL). $NEt_3H^+Cl^-$ immediately precipitated. The reaction mixture was stirred at room temperature for 10 h and was then poured into water (40 mL). The mixture was extracted three times with Et_2O (30 mL each), and the organic extracts were dried over $MgSO_4$. After filtration and removal of the solvent by rotary evaporation, the resulting slightly yellowish oil was passed through a short column of alumina using hexanes as the eluant to yield 1.0 g (92%) of 5-{[[11′-[2″,5″-bis[2-(3′-fluoro-4′-methoxyphenyl)ethynyl]phenyl]undecyl]oxy]carbonyl}bicyclo[2.2.1]hept-2-ene. The monomer was purified for polymerization by recrystallization from Et_2O/methanol outside of the drybox and from hexanes in the drybox; 78% endo. ^{1}H NMR: 1.90 (m), 2.21 (m), 2.92 (s), 2.95 (m), 3.02 (s), and 3.20 (s) are due to the nonolefinic norbornene protons of both isomers which are not buried under the resonances of the undecyl spacer; 1.27 (m, $-[CH_2]_7-$), 1.55 (m, $-CH_2CH_2O_2C-$), 1.70 (m, $-CH_2CH_2Ar$), 2.82 (t, $-CH_2Ar$), 3.92 (s, $-OCH_3$, 6 H), 4.00 (t, $-CH_2O_2C-$), 5.92 (m, 1 olefinic H, endo), 6.12 (m, 2 olefinic H, exo), 6.18 (1 olefinic H, endo), 6.93 (ddd, 2 aromatic H ortho to $-OCH_3$), 7.24 (m, 4 aromatic H meta to $-OCH_3$), 7.30 (dd, 1 aromatic H para to $-CH_2-$), 7.37 (d, 1 aromatic H ortho to $-CH_2-$), 7.44 (d, 1 aromatic H meta to $-CH_2-$). Anal. ($C_{43}H_{46}F_2O_4$) C, H: calcd, 77.68, 6.97; found, 77.43, 7.23.

5-{[[11′-[2″,5″-Bis[2-(3′-fluoro-4′-ethoxyphenyl)ethynyl]phenyl]undecyl]oxy]carbonyl}bicyclo[2.2.1]hept-2-ene (85% endo). ^{1}H NMR: 1.89 (m), 2.21 (m), 2.91 (s), 2.92 (m), 3.02 (s), and 3.20 (s) are the resolved resonances of the nonolefinic norbornene protons of both isomers; 1.27 (m, $-[CH_2]_7-$), 1.47 (t, $-CH_3$, 6 H), 1.58 (m, $-CH_2CH_2O_2C-$, 4 H), 1.69 (m, $-CH_2CH_2Ar$), 2.81 (t, $-CH_2Ar$), 4.01 (m, $-CH_2O_2C-$), 4.14 (q, $-CH_2OAr$, 4 H), 5.91 (m, 1 olefinic H, endo), 6.12 (m, 2 olefinic H, exo), 6.18 (1 olefinic H, endo), 6.92 (ddd, 2 aromatic H ortho to $-OCH_2-$), 7.24 (m, 4 aromatic H meta to $-OCH_2-$), 7.30 (dd, 1 aromatic H para to $-CH_2-$), 7.36 (d, 1 aromatic H ortho to $-CH_2-$), 7.43 (d, 1 aromatic H meta to $-CH_2-$). Anal. ($C_{45}H_{50}F_2O_4$) C, H: calcd, 78.01, 7.27; found, 77.68, 7.43.

5-{[[11′-[2″,5″-Bis[2-(3′-fluoro-4′-*n*-propoxyphenyl)ethynyl]phenyl]undecyl]oxy]carbonyl}bicyclo[2.2.1]hept-2-ene (73% endo). ^{1}H NMR: 2.21 (m), 2.89 (s), 2.94 (m), 3.02 (s), and 3.19 (s) are the resolved resonances of the nonolefinic norbornene protons of both isomers; 1.06 (t, $-CH_3$, 6 H), 1.27 (m, $-[CH_2]_7-$), 1.59 (m, $-CH_2CH_2O_2C-$, 4 H), 1.70 (m, $-CH_2CH_2Ar$), 1.86 (m, $-CH_2CH_2OAr$, 4 H), 2.81 (t, $-CH_2Ar$), 4.02 (m, $-CH_2OAr$ and $-CH_2O_2C-$, 6 H), 5.92 (m, 1 olefinic H, endo), 6.12 (m, 2 olefinic H, exo), 6.19 (1 olefinic H, endo), 6.92 (ddd, 2 aromatic H ortho to $-OCH_2-$), 7.23 (m, 4 aromatic H meta to $-OCH_2-$), 7.32 (dd, 1 aromatic H para to $-CH_2-$), 7.36 (d, 1 aromatic H ortho to $-CH_2-$), 7.43 (d, 1 aromatic H meta to $-CH_2-$). Anal. ($C_{47}H_{54}F_2O_4$) C, H: calcd, 78.30, 7.55; found, 78.13, 7.60.

5-{[[11′-[2″,5″-Bis[2-(3′-fluoro-4′-*n*-butoxyphenyl)ethynyl]phenyl]undecyl]oxy]carbonyl}bicyclo[2.2.1]hept-2-ene (75% endo). ^{1}H NMR: 1.89 (m), 2.21 (m), 2.90 (s), 2.94 (m), 3.03 (s), and 3.20 (s) are the resolved resonances of the nonolefinic norbornene protons of both isomers; 0.99 (t, $-CH_3$, 6 H), 1.26 (m, $-[CH_2]_7-$), 1.54 (m, $-CH_2CH_2O_2C-$ and $-CH_2[CH_2]_2O-$, 6 H), 1.69 (m, $-CH_2CH_2Ar$), 1.82 (m, $-CH_2CH_2OAr$, 4 H), 2.81 (t, $-CH_2Ar$), 4.00 (q, $-CH_2O_2C-$), 4.06 (t, $-CH_2OAr$, 4 H), 5.92 (m, 1 olefinic H, endo), 6.12 (m, 2 olefinic H, exo), 6.19 (1 olefinic H, endo), 6.92 (ddd, 2 aromatic H ortho to $-OCH_2-$), 7.22 (m, 4 aromatic H meta to $-OCH_2-$), 7.30 (dd, 1 aromatic H para to $-CH_2-$), 7.36 (d, 1 aromatic H ortho to $-CH_2-$), 7.43 (d, 1 aromatic H meta to $-CH_2-$). Anal. ($C_{49}H_{58}F_2O_4$) C, H: calcd, 78.58, 7.81; found, 78.15, 7.95.

The ^{1}H NMR spectra of the 5-{[[11′-[2″,5″-bis[2-(3′-fluoro-4′-*n*-alkoxyphenyl)ethynyl]phenyl]undecyl]oxy]carbonyl}bicyclo[2.2.1]hept-2-enes with $n = 5-12$ are identical. ^{1}H NMR: 1.88 (m), 2.21 (m), 2.91 (s), 2.94 (m), 3.03 (s), and 3.20 (s) are the resolved resonances of the nonolefinic norbornene protons of both isomers; 0.90 (t, $-CH_3$, 6 H), 1.15−1.60 (m, $-[CH_2]_8-$ and $-[CH_2]_{n-3}CH_2CH_2O_2C-$, $4n + 4$ H), 1.69 (m, $-CH_2CH_2Ar$), 1.83 (m, $-CH_2CH_2OAr$, 4 H), 2.81 (t, $-CH_2Ar$), 4.00 (q, $-CH_2O_2C-$), 4.05 (t, $-CH_2OAr$, 4 H), 5.92 (m, 1 olefinic H, endo), 6.12 (m, 2 olefinic H, exo), 6.18 (1 olefinic H, endo), 6.92 (ddd, 2 aromatic H ortho to $-OCH_2-$), 7.23 (m, 4 aromatic H meta to $-OCH_2-$), 7.30 (dd, 1 aromatic H para to $-CH_2-$), 7.36 (d, 1 aromatic H ortho to $-CH_2-$), 7.43 (d, 1 aromatic H meta to $-CH_2-$). Anal. ($C_{51}H_{62}F_2O_4$, 67% endo) C, H: calcd, 78.83, 8.04; found, 78.62, 8.19. Anal. ($C_{53}H_{66}F_2O_4$, 67% endo) C, H: calcd, 79.07, 8.26; found, 78.78, 8.37. Anal. ($C_{55}H_{70}F_2O_4$, 57% endo) C, H: calcd, 79.29, 8.47; found, 79.50, 8.49. Anal. ($C_{57}H_{74}F_2O_4$, 67% endo) C, H: calcd, 79.50, 8.66; found, 79.36, 8.82. Anal. ($C_{59}H_{78}F_2O_4$, 50% endo) C, H: calcd, 79.69, 8.84; found, 79.51, 9.08. Anal. ($C_{61}H_{82}F_2O_4$, 60% endo) C, H: calcd, 79.87, 9.01; found, 80.07, 9.12. Anal. ($C_{63}H_{86}F_2O_4$, 67% endo) C, H: calcd, 80.04, 9.17; found, 80.20, 9.40. Anal. ($C_{65}H_{90}F_2O_4$, 67% endo) C, H: calcd, 80.20, 9.32; found, 80.31, 9.55.

Polymerizations. In a typical procedure, a solution of 5-{[[11′-[2″,5″-bis[2-(3′-fluoro-4′-methoxyphenyl)ethynyl]phenyl]undecyl]oxy]carbonyl}bicyclo[2.2.1]hept-2-ene (0.34 g, 0.51 mmol) in dry THF (3.9 g) was added dropwise over 1 min to a solution of $Mo(CHCMe_2Ph)(N\text{-}2,6\text{-}{}^iPr_2Ph)(O^tBu)_2$ (5.5 mg, 1.0 μmol) in dry THF (1.1 g). After stirring at room temperature for 2 h, the orange solution was quenched with benzaldehyde (15 μL, 0.15 mmol) and then stirred for 10 min. The solution was taken outside of the drybox and precipitated in methanol (100 mL). The precipitate was collected, reprecipitated from THF (10 mL) into methanol (100 mL), and dried to yield 0.29 g (88%) of polymer as a coagulated solid; $M_n = 4.4 \times 10^4$, $M_w/M_n = 1.17$.

Acknowledgment is made to the donors of the Petroleum Research Fund, administered by the American Chemical Society, for support of this research. C.P. also acknowledges the National Science Foundation for an NSF Young Investigator Award (1994−1999) and matching funds from Bayer, Dow Chemical, DuPont (DuPont Young Professor Grant), GE Foundation (GE Junior Faculty Fellowship), Pharmacia Biotech, and Waters Corp.

Supporting Information Available: Differential scanning calorimetry traces of the {2,5-bis[(3′-fluoro-4′-*n*-alkoxyphenyl)ethynyl]phenyl}undecane model compounds (1 page). Ordering information is given on any current masthead page.

References and Notes

(1) Demus, D.; Zaschke, H. *Flussige Kristalle in Tabellen II*; VEB Deutscher Verlag: Leipzig, Germany, 1984.

(2) Pugh, C.; Andersson, S. K.; Percec, V. *Liq. Cryst.* **1991**, *10*, 229.

(3) Pugh, C.; Dharia, J.; Arehart, S. V. *Macromolecules* **1997**, *30*, 4520.

(4) (a) Pugh, C.; Arehart, S.; Liu, H.; Narayanan, R. *J. Macromol. Sci., Pure Appl. Chem.* **1994**, *A31*, 1591. (b) Pugh, C.; Liu, H.; Arehart, S. V.; Narayanan, R. *Macromol. Symp.* **1995**, *98*, 293.

(5) (a) Zhou, Q.-F.; Li, H.-M.; Feng, X.-D. *Macromolecules* **1987**, *20*, 233. (b) Zhou, Q.-F.; Li, H.-M.; Feng, X.-D. *Mol. Cryst. Liq. Cryst.* **1988**, *155*, 73. (c) Keller, P.; Hardouin, F.; Mauzac, M.; Achard, M. F. *Mol. Cryst. Liq. Cryst.* **1988**, *155*, 171. (d) Gray, G. W.; Hill, J. S.; Lacey, D. *Angew. Chem., Int. Ed. Engl.* **1989**, *28*, 1120. (e) Hardouin, F.; Mery, S.; Achard, M. F.; Mauzac, M.; Davidson, P.; Keller, P. *Liq. Cryst.* **1990**, *8*, 565. (f) Leube, H. F.; Finkelmann, H. *Makromol. Chem.* **1990**, *191*, 2707. (g) Lewthwaite, R. A.; Gray, G. W.; Toyne, K. J. *J. Mater. Chem.* **1992**, *2*, 119. (h) Percec, V.; Tomazos, D. *J. Mater. Chem.* **1993**, *3*, 643. (i) Achard, M. F.; Lecommandoux, S.; Hardouin, F. *Liq. Cryst.* **1995**, *19*, 581. (j) Takenaka, S.; Yamasaki, K. *Mol. Cryst. Liq. Cryst.* **1995**, *258*, 51. (k) Leroux, N.; Chien, L.-C. *Liq. Cryst.* **1996**, *21*, 189.

(6) (a) Hessel, F.; Finkelmann, H. *Polym. Bull.* **1985**, *14*, 375. (b) Hessel, F.; Herr, R.-P.; Finkelmann, H. *Makromol. Chem.* **1987**, *188*, 1597. (c) Hessel, F.; Finkelmann, H. *Makromol. Chem.* **1988**, *189*, 2275. (d) Leube, H. F.; Finkelmann, H. *Makromol. Chem.* **1991**, *192*, 1317.

(7) Cherodian, A. S.; Hughes, N. J.; Richardson, R. M.; Lee, M. S. K.; Gray, G. W. *Liq. Cryst.* **1993**, *14*, 1667.

(8) (a) Hardouin, F.; Mery, S.; Achard, M. F.; Noirez, L.; Keller, P. *J. Phys. II* **1991**, *1*, 511 and Erratum 871. (b) Hardouin, F.; Leroux, N.; Mery, S.; Noirez, L. *J. Phys. II* **1992**, *2*, 271. (c) Leroux, N.; Keller, P.; Achard, M. F.; Noirez, L.; Hardouin, F. *J. Phys. II* **1993**, *3*, 1289.

(9) Lecommandoux, S.; Achard, M. F.; Hardouin, F.; Brület, A.; Cotton, J. P. *Liq. Cryst.* **1997**, *22*, 549.

(10) Arehart, S. V.; Pugh, C. *J. Am. Chem. Soc.* **1997**, *119*, 3027.

(11) Pugh, C.; Bae, J.-Y.; Dharia, J.; Ge, J. J.; Cheng, S. Z. D. *Macromolecules*, submitted.

(12) Pugh, C.; Schrock, R. R. *Macromolecules* **1992**, *25*, 6593.

(13) Pugh, C.; Kiste, A. L. *Prog. Polym. Sci.* **1997**, *22*, 601.

(14) Ungerank, M.; Winkler, B.; Eder, E.; Stelzer, F. *Macromol. Chem. Phys.* **1995**, *196*, 3623.

(15) Komiya, Z.; Schrock, R. R. *Macromolecules* **1993**, *26*, 1393.

(16) Hawthorne, M. F.; Reintjes, M. *J. Am. Chem. Soc.* **1965**, *87*, 4585.

(17) Ritter, K. *Synthesis* **1993**, 735 and references therein.

(18) Stang, P. J.; Hanack, M.; Subramanian, L. R. *Synthesis* **1982**, 85 and references therein.

(19) (a) Gray, G. W.; Goodby, J. W. *Smectic Liquid Crystals. Textures and Structures*; Leonard Hall: Glasgow, U.K., 1984. (b) Demus, D.; Richter, L. *Textures of Liquid Crystals*; Verlag Chemie: Weinheim, Germany, 1978.

(20) See for example: Komiya, Z.; Pugh, C.; Schrock, R. R. *Macromolecules* **1992**, *25*, 6586.

(21) (a) Demus, D.; Diele, S.; Hauser, A.; Latif, I. Selemann, C.; Weissflog, W. *Cryst. Res. Technol.* **1985**, *20*, 1547. (b) Weissflog, W.; Demus, D. *Mol. Cryst. Liq. Cryst.* **1985**, *129*, 235. (c) Perez, F.; Berdagué, P.; Judeinstein, P.; Bayle, J. P.; Allouchi, H.; Chasseau, D.; Cotrait, M.; Lafontaine, E. *Liq. Cryst.* **1995**, *19*, 345. (d) Berdagué, P.; Perez, F.; Bayle, J. P.; Ho, M.-S.; Fung, B. M. *New J. Chem.* **1995**, *19*, 383.

(22) Jacobine, A. F.; Glaser, D. M.; Nakos, S. T. *Polym. Mater. Sci. Eng.* **1989**, *60*, 211.

(23) (a) Pugh, C.; Percec, V. *Chem. Mater.* **1991**, *3*, 107. (b) Pugh, C.; Percec, V. *J. Polym. Sci., Polym. Chem. Ed.* **1990**, *28*, 1101.

(24) (a) Schrock, R. R.; Murdzek, J. S.; Bazan, G. C.; Robbins, J.; DiMare, M.; O'Regan, M. *J. Am. Chem. Soc.* **1990**, *112*, 3875. (b) Fox, H. H.; Yap, K. B.; Robbins, J.; Cai, S.; Schrock, R. R. *Inorg. Chem.* **1992**, *31*, 2287.

MA9715738